2001: The Journal of Astronomical Data 7, 1.

Luminosities of [O III] λ5007 and Hydrogen Balmer lines in nova shells years and decades after outburst

Ronald A. Downes (1)* and Hilmar W. Duerbeck (2)†
with the collaboration of
Cathérine E. Delahodde (3)†
(1) Space Telescope Science Institute, 3700 San Martin Drive, Baltimore, MD 21218, USA
(2) University of Brussels (VUB), Pleinlaan 2, 1050 Brussels, Belgium
(3) European Southern Observatory, A. de Cordova 3107, Santiago, Chile
(now at Institut d'Astrophysique de Marseille, Traverse du Siphon,
F-13376 Marseille Cedex 12, France)

Received November 2001; accepted December 2001

Abstract

The evolution of the luminosity of nova shells in the century following the nova outburst is studied for the lines Hα, Hβ, and [O III] λ5007. About 1200 flux measurements from 96 objects have been collected from the literature, from unpublished observations, from the HST archive, or from new narrow-band filter imaging. For most objects, the distance and reddening is known (or newly determined), and luminosities were calculated from the observed fluxes. The luminosity data were combined in five groups, according to nova light curve type (very fast, fast, moderately fast, slow, recurrent); some objects were re-assigned to other groups for a better fit of the luminosity data to the general trend.

For very fast, fast and moderately fast novae, the slope of the [O III] λ5007 decline is very similar, leading to a basic 'switchoff' of [O III] λ5007 emission after 11, 23 and 24 years, respectively. For the same speed classes, the slope of the Balmer luminosity is quite similar.

In contrast to all types of fast novae, the decline in Balmer luminosity is more rapid in slow novae. However, the slope in [O III] λ5007 is more gentle; slow novae still show [O III] λ5007 emission after 100 years. Thus shells of slow novae are still hot after one century; the same applies for the shells of the very fast nova GK Per and the recurrent nova T Pyx, which interact with circumstellar material.

In recurrent novae, [O III] λ5007 is usually inconspicuous or absent. In objects with giant companions, the Balmer luminosity decreases very slowly after an outburst, which may be

*Visiting Astronomer, Kitt Peak National Observatory, National Optical Astronomy Observatories, which is operated by the Association of Universities for Research in Astronomy, Inc. under contract with the National Science Foundation

†Based on observations collected at the European Southern Observatory, La Silla, Chile

an effect of line blending of material from the ejecta and the giant wind. On the other hand, objects with dwarf companions show a very rapid decline in Balmer luminosity.

Keywords: novae: shells, novae: decline, cataclysmic variables

1 Introduction

In the past years and decades, several models of nova shells have been presented in the literature. Often they were adapted to describe the state and evolution of specific objects, and often remarkable agreement between model and observation was achieved. Nevertheless it should be kept in mind that a nova shell is a rapidly evolving object, and its properties change significantly with time. Furthermore, a plethora of different types of novae are observed, which is accompanied by an amazing variety of nova shells of various morphologies and physical properties in different stages of temporal development.

Although studies of nova shells have been carried out since the first bright nova of the 20th century, GK Persei in 1901, most of these studies were carried out in a qualitative way. This approach permitted the calculation of nebular expansion parallaxes and the morphological study of shells. Since the shells were usually faint, and the observations were carried out with photographic plates, hardly any quantitative results are available. Only in the first phases of the outburst, when the shells document themselves in the form of emission lines, were the line fluxes estimated and derived for a few cases, notably by Payne-Gaposchkin and collaborators. Replacement of the photographic plate by digital receivers has facilitated the task of studying the evolution of nova remnants, both spectroscopically and by means of direct imaging through narrow-band filters. In fact, quite a number of studies have even been carried out for extragalactic novae, where Hα-images can more easily detect the objects above the stellar background (see, e.g. Ciardullo et al. 1987).

In this paper, we report on the results of a recent imaging survey of nova remnants, carried out at the Kitt Peak and ESO La Silla observatories. We also use a hitherto unpublished survey of nova shells carried out in 1984 at Calar Alto, and the images from the *Hubble Space Telescope* archive. Furthermore, we have collected and homogenized the existing quantitative record of nova shell observations. Because the survey attempted to cover as many objects in as many evolutionary stages as possible, hardly any detailed information on a given object, or any detailed modelling of shells will be given (i.e. the distribution of line flux between various specific parts of a nova shell). We rather attempt to describe the "average" or global evolutionary track of a nova shell, in order to derive expected values for faint shells of ancient novae. A theoretical interpretation of the observed behavior will be the subject of a forthcoming paper (Duerbeck & Downes 2002).

Section 2 describes our observations and reductions. Section 3 briefly describes the classification of novae according to speed class, which is the base for merging our shell luminosity data into groups. Section 4 gives the derivation of global trends in luminosity evolution for the lines Hα, Hβ and [O III] λ5007 in novae of different speed classes (including, besides classical novae, recurrent ones). Section 5 summarizes our results.

2 Observations

Old data of nova shell line fluxes, derived both from spectral observations or direct images, were collected from the literature. Besides many data scattered in the literature, the early photographic studies of Payne-Gaposchkin and collaborators deserve special mentioning, as

well as the recent Tololo nova survey, carried out by Williams and collaborators, and kindly put at our disposal by him.

The new observations were obtained at the European Southern Observatory, La Silla, Chile, and at the the Kitt Peak National Observatory. On 1998 March 21 – 23, the Dutch 0.9 m telescope at ESO, equipped with a TEK TK512CB chip (512 × 512 pixels) with a scale of $0\farcs465$ pixel^{-1} was used. On 1998 May 28 – June 1, observations were obtained with the KPNO 2.1 m telescope using the TEK "T1KA" chip (1024 × 1024 pixels with a scale of $0\farcs305$ pixel^{-1}), and on 1998 June 30 with the KPNO 0.9 m telescope using the TEK "T2KA" chip (2048 × 2048 pixels with a scale of $0\farcs7$ pixel^{-1}). A final run was carried out at the Danish 1.54 m telescope at ESO on 2000 July 16. The DFOSC was used, which has a LORAL/LESSER chip (2052 × 2052 pixels with a scale of $0\farcs39$ pixel^{-1}).

The data were obtained with narrow-band filters centered at Hα (80 and 62 Å FWHM at the ESO Dutch and Danish, 36Å at KPNO) and [O III] λ5007 (55 and 57Å at the ESO Dutch and Danish, 31Å at KPNO), as well as off-band and *UBVR* filters; see Downes & Duerbeck (2000) for details. Note that the offband [O III] λ5007 filter for the objects observed at ESO is a Strömgren y filter. The data were reduced in the standard manner.

Flux calibration of the novae were obtained via "standard" planetary nebulae. NGC 6833 was used for the KPNO observations. The Hα and [O III] flux of NGC 6833 was determined by Tony Keyes (private communication) based on *Hubble Space Telescope* Faint Object Spectrograph observations, and we adopted values of 3.9×10^{-12} erg cm^{-2} s^{-1} arcsec^{-2} and 9.4×10^{-12} erg cm^{-2} s^{-1} arcsec^{-2} for Hα and [O III], respectively. For the "Dutch" observations, Sp 1 was used. The Hα and [O III] flux of Sp 1 was measured by Perinotto et al. (1994) and the authors of the Strasbourg/ESO catalog of galactic planetary nebulae (Acker et al. 1992) spectroscopically, and by Webster (1969), Copetti (1990) and Shaw & Kaler (1989) through interference filters. Unfortunately, the results show some scatter, so we assume fluxes of $2.6 \pm 0.5 \times 10^{-11}$ erg cm^{-2} s^{-1} arcsec^{-2} and $2.8 \pm 0.2 \times 10^{-11}$ erg cm^{-2} s^{-1} arcsec^{-2} for Hα and [O III], respectively. For the "Danish" observations, three objects from the list of Dopita & Hua (1997) were used: PN 327.5+13.3, PN 327.1−01.8, and PN 321.3−16.7.

On the second night of the ESO "Dutch" observations, the flux of Sp 1 was fainter by $0\fm38$ and $0\fm28$ in Hα and [O III], an effect that was traced in the magnitudes of stars measured in these filters as well. Thus, we assume that the overall transmission, and not the central wavelength, underwent a change. Broadband transmission was very similar in the three nights. We thus took the nightly aperture magnitude of the PN, corrected to airmass 1, as the "zero-point" of the system, which corresponds to the fluxes given.

The targets were partly starlike, and normal DAOPHOT photometry was carried out for most of the nebulae. In the [O III] data, V842 Cen and V1974 Cyg were slightly resolved, and RR Pic and CP Pup were clearly resolved (Downes & Duerbeck 2000). In these cases, the onband and offband frames were aligned, the offband frame scaled appropriately to cancel the majority of stars, and subtracted from the onband frame. In most cases, a starlike center remained (because of emission in the region of [O III]), and this central emission was again fitted with a psf-profile of the onband frame, yielding an emission-line magnitude of the central star. The detached nebular shell emission was measured in an annulus, where the central "remnant" that remained from the subtraction and fitting attempts, was duly neglected. More objects were slightly resolved in Hα, and a similar process was performed.

For the starlike images, the nova magnitudes measured from the images are a combination of the line flux from the shell plus a continuum flux from the stellar remnant. This continuum flux needs to be removed if we are to study the Hα and [O III] λ5007 line fluxes themselves. To correct for the continuum flux, a fit was made to all objects (excluding the nova) in the

field of the form

$$\text{onband} - \text{magnitude} = a_0 + a_1 \times \text{offband} - \text{magnitude}.$$

These fits allowed us to estimate the flux in the continuum of the novae, and thus to derive net line fluxes.

For the ESO observations, the use of the broad-band Strömgren y filter as the [O III] off-band resulted in a more involved continuum removal. We note that this filter has practically the same central wavelength as a broadband Johnson V filter, without, however, including strong emission lines like the [O III] lines. For all field stars, V magnitudes in the standard system are available. The magnitude difference for the V- and the (uncalibrated) y-observations was determined, by establishing the relation

$$y = V + V_0,$$

i.e. by determining the zero-point difference V_0. Furthermore, for all stars (excluding the nova) the relation

$$m_{\text{O III}} = y + y_0$$

was established and y_0 determined. Thus the magnitude difference between the V magnitude and the [O III]-magnitude of an object without emission lines is

$$m_{\text{O III}} = V + V_0 + y_0.$$

Field stars of all colours scatter from these linear relations by $\pm 0\overset{\text{m}}{.}01$ to $0\overset{\text{m}}{.}02$, including M-stars with TiO bands. Thus it is likely that unusually blue stars (like nova star continua in their late stages) also will not deviate significantly.

Under this assumption, the presumably emission-free y magnitude of the nova was used to calculate its hypothetical "emission-free" V-magnitude, and from this magnitude, its "emission-free" [O III]-magnitude was derived. The flux corresponding to this magnitude was subtracted from the flux calculated from the observed [O III]-magnitude, yielding an "emission-only" [O III] flux. In most cases, the correction due to stellar contamination was below 10% of the total flux.

We also evaluated direct images of nova shells, taken in August 1984 through Hα and [O III] λ5007 filters, with a CCD camera in the Cassegrain focus of the Calar Alto 2.2m telescope (operated by the Centro Astronomico Hispano-Aleman, Almeria, and the Max-Planck Institut für Astronomie, Heidelberg; observers were H.W. Duerbeck and W.C. Seitter). Only resolved shells were considered, the central stars (and others in the field) were reduced with the DAOPHOT allstar routine within IRAF, and aperture photometry was carried out using MIDAS. The planetary nebula M57 (NGC 6720) served as a flux standard.

Furthermore, we used flux-calibrated spectroscopic observations of several novae, taken (by us) at several telescopes in the past 25 years. Determination of the [O III] λ5007 and Hα fluxes was straightforward, since the shells were usually unresolved. We were also given access to the extensive data set obtained in the Tololo Nova Survey (cf. Williams et al. 1994), from which direct line flux measurements were made.

In addition to the ground-based data, we used archival [O III] λ5007 and Hα images obtained with the *Hubble Space Telescope*. Finally, we collected shell fluxes from the literature, which were derived from direct images or spectroscopy of nova shells.

To be able to compare line strengths from different objects, we converted the observed fluxes to luminosities; the distances and reddenings necessary for the conversion were mostly taken from Downes & Duerbeck (2000); a few additional determinations or re-determinations are discussed in the Appendix of this paper. The list of objects, with adopted distances,

reddenings, and references to these data, as well as references for the flux measurements, is given in Table 1. The complete set of data are given in Table 2, Table 3 and Table 4 for [O III] λ5007, Hα, and Hβ, respectively.

3 Nova groupings

In order to merge sparse observations of many objects into a single diagram, a reasonable grouping of objects seems desirable. Since the photospheric growth and shrinking is controlled by the mass loss in the course of the outburst, and the photospheric shrinking is reflected in the light curve, we have found it appropriate to sort the data according to nova speed class.

The speed classes adopted were those defined in Payne-Gaposchkin (1957): very fast, fast, moderately fast, slow and very slow, depending on the average decline rate over the first two magnitudes (t_2). Her classification supersedes previous schemes by McLaughlin (1939) (fast, average, slow, RT Ser-type) and Bertaud (1948) (fast, slow, very slow), which were usually based on t_3 times. However, Payne-Gaposchkin's classification can lead to serious errors in some slow novae which show a pronounced maximum of somewhat more than two magnitudes, superimposed on a plateau of almost constant brightness (e.g. RR Pic). In a few cases, we have deliberately modified the assignment to group together similar objects. Similarly, a few reassignments were made to better fit the shell flux data of a single object to the general trend prevailing in a neighboring speed class. Such reassignments are noted below.

In addition to the speed classes, we have also tried to discriminate between the spectral classes Fe- and He/N novae according to the criteria given by Williams (1992); a source of this information is Della Valle & Livio (1998). Finally, confirmed and probable ONeMg novae were identified, either from recent work in the literature, or from earlier descriptions (for an early identification of such objects, see McLaughlin (1944)).

The objects for which shell flux data were obtained are listed in Table 1, together with decline times t_2, t_3, speed class, spectral class, and peculiarity (i.e. ONeMg group, recurrent nova, or nova with noticeable dust formation).

4 Line emission as a function of time

The nova distances and reddenings of Table 1 and the observed nova fluxes of Tables 2, 3 and 4 were used to calculate line luminosities, which are also given in Tables 2, 3 and 4. Depending on the distance, reddening and type of nova, the luminosity of the stellar remnant, as well as the light gathering and resolving power of the telescope used for the study, there is a lower limit for the line luminosity that can still be recorded with certainty. In general, we have assumed a luminosity of 10^{30} erg s^{-1} as the lower limit that was achieved with the telescopes used in this study. This should be regarded as an averaged a posteriori value. To derive a correct estimate of the lower limit, one would not only have to take into account the distance, but also source confusion in the case of an extended shell, and the contribution of accretion disk emission in the case of a pointlike object. In the following, the nova is said to have "switched off" emission in a specific line if its luminosity was below the value 10^{30} erg s^{-1}.

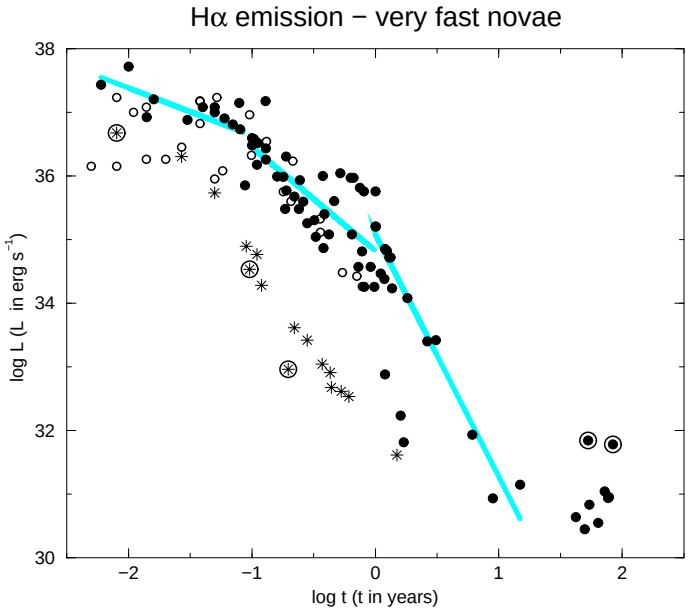

Figure 1: Hα luminosity versus time for very fast novae. Galactic novae are shown as filled circles, extragalactic novae as open circles. The unusual objects V838 Her and V4160 Sgr are shown with asterisks/encircled asterisks, respectively. The recent fluxes of GK Per and CP Pup are shown as encircled filled circles near abscissa value 2 (GK Per is the rightmost symbol).

4.1 Very fast novae

The behavior of very fast novae is illustrated in Figs. 1 – 3. In these diagrams, the logarithm of the luminosity (measured in ergs s^{-1}) is plotted versus logarithm of time after maximum (time measured in years). Ordinary galactic novae are shown as filled circles, and relations are determined exclusively for this galactic dataset, unless stated otherwise. Extragalactic novae are shown as open circles, and are merely displayed for comparison. Unusual novae (mentioned in the text and the figure caption) are shown with special symbols.

4.1.1 Hα

The Hα evolution of very fast novae appears to be quite homogeneous, unlike the evolution of the other spectral lines considered below. Several objects, however, have to be considered separately. One is M31-C31, which is similar in evolution than the other novae, but systematically fainter at earlier stages (see below). The long series of measurements of V838 Her (indicated as asterisks in Figs. 1–3) shows that it is much fainter and faster in its evolution than other very fast novae, except V4160 Sgr, which is marked with encircled asterisks.

Many of the famous bright novae of the 20th century (V603 Aql, GK Per and CP Lac) are not present in this diagram, since no spectrophotometry was obtained longward of the photographic (blue) region.

The general evolution can be approximated by straight lines. At times $-2.5 < \log t < -1.0$ (< 10 days), the novae have

$$\log(L_{\mathrm{H}\alpha}) = \underset{\pm 0.38}{35.89} - \underset{\pm 0.25}{0.75} \log\ (\mathrm{age}),$$

or an almost constant luminosity,

$$\log(L_{\mathrm{H}\alpha}) \approx 37.0 \pm 0.4 \text{ ergs s}^{-1}.$$

At times $-1.0 < \log t < 0.0$ (10 days to 1 year)

$$\log(L_{\mathrm{H}\alpha}) = \underset{\pm 0.15}{34.82} - \underset{\pm 0.25}{1.63} \log\ (\mathrm{age})$$

and at late times ($0.0 < \log t < 1.5$):

$$\log(L_{\mathrm{H}\alpha}) = \underset{\pm 0.11}{35.08} - \underset{\pm 0.24}{3.81} \log\ (\mathrm{age}).$$

The fit was restricted to $\log t < 1.5$, since at very late times emission from the accretion disk may contaminate the measurements. A few points were omitted, which belong to single, poorly-observed objects.

The data points of V838 Her lie all on a straight line which can be approximated by

$$\log(L_{\mathrm{H}\alpha}) = \underset{\pm 0.07}{31.88} - \underset{\pm 0.09}{2.83} \log\ (\mathrm{age}).$$

The class of 'superbright novae' (V1500 Cyg, N LMC 1991) by Della Valle (1991) is not obvious in the present diagrams. If there is anything peculiar, it is the *faintness* of M31-C31. Since Della Valle used the M31 novae as a template (and M31-C31 appears to fit well into this group), it appears that *all* very fast galactic novae fall into the region of the superbright novae, a fact also clearly seen in the S-calibration of Downes & Duerbeck (2000), as applied to Galactic novae. Why there is such a marked discrepancy in the observed behaviour of very fast novae in the Galaxy and in M31 remains to be explained.

At late times (typically $\log t = 1.75$, i.e. 50 years after outburst), fast novae still show Hα emission at a level of a few $\times 10^{30}$ ergs s^{-1}. Two objects, however, are noticeably brighter: CP Pup and GK Per. It is obvious that the emission does not originate from the accretion disk, since the shell is spatially resolved.

4.1.2 Hβ

The Hβ flux shows a large scatter (this is possibly due to the fact that the old novae V603 Aql, GK Per, CP Lac etc. are now included). It appears as if there are two well-defined bands, an upper and a lower one, with only a few points in between. The extragalactic (LMC, M31) novae seem to cluster near the lower band. As in the previous diagram, V838 Her is notably fainter than the rest.

As in the case of Hα, between $\log t = -2$ and -1.5 (i.e. 1 day and 15 days after maximum), flux levels are almost constant at 10^{36} and 10^{38} ergs s^{-1} ($< \log L >= 36.91 \pm 0.71$ ergs s^{-1}); afterwards, a decline sets in. At times $-2.5 < \log t < -1.0$

$$\log(L_{\mathrm{H}\beta}) = \underset{\pm 0.52}{35.90} - \underset{\pm 0.35}{0.53} \log\ (\mathrm{age}).$$

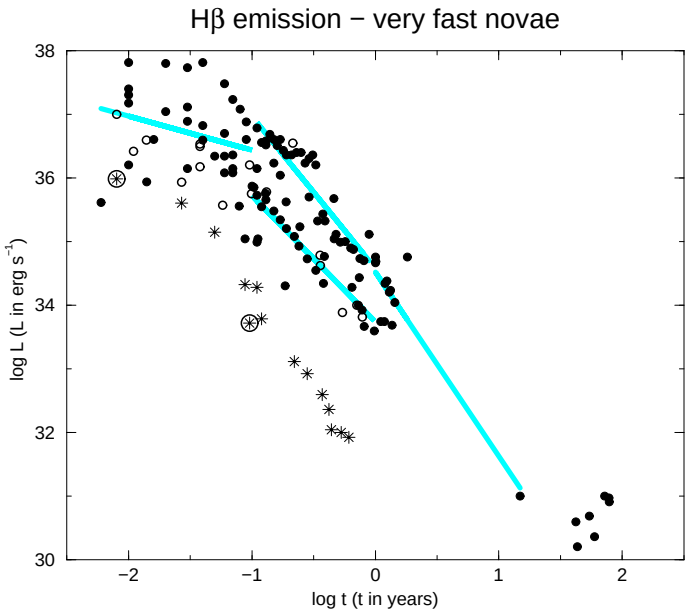

Figure 2: Hβ luminosity versus time for very fast novae. Galactic novae are shown as filled circles, extragalactic novae as open circles. The unusual objects V838 Her and V4160 Sgr are shown with asterisks/encircled asterisks, respectively.

At times $-1.0 < \log t < 0.0$, a dichotomy seems indicated. The upper line is

$$\log(L_{\mathrm{H}\beta}) = \underset{\pm 0.11}{34.57} - \underset{\pm 0.18}{2.39} \log\ (\mathrm{age}),$$

and the lower one

$$\log(L_{\mathrm{H}\beta}) = \underset{\pm 0.14}{33.74} - \underset{\pm 0.20}{1.98} \log\ (\mathrm{age}).$$

At late times ($0.0 < \log t < 1.5$), the slope is only poorly documented, and at times $\log t > 1.5$, emission from the disk may dominate. The slope at late times is:

$$\log(L_{\mathrm{H}\beta}) = \underset{\pm 0.14}{34.52} - \underset{\pm 0.40}{2.89} \log\ (\mathrm{age}).$$

The time interval $(-1.0, 1.0)$ can also be fitted with one straight line:

$$\log(L_{\mathrm{H}\beta}) = \underset{\pm 0.18}{34.35} - \underset{\pm 0.27}{1.94} \log\ (\mathrm{age}).$$

Finally, the nova V838 Her follows its own relation:

$$\log(L_{\mathrm{H}\beta}) = \underset{\pm 0.08}{31.25} - \underset{\pm 0.10}{2.90} \log\ (\mathrm{age}).$$

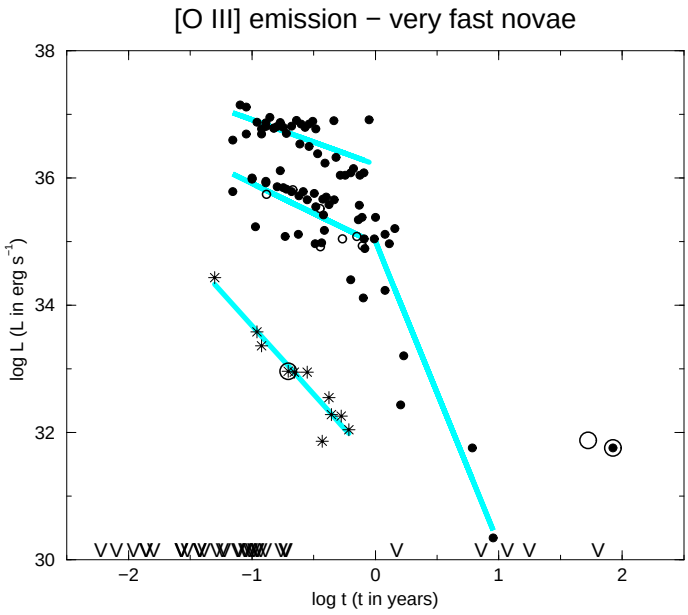

Figure 3: [O III] λ5007 luminosity versus time for very fast novae. Galactic novae are shown as filled circles, extragalactic novae as open circles. The unusual objects V838 Her and V4160 Sgr are shown with asterisks/encircled asterisks, respectively. The recent luminosity of GK Per is shown as an encircled filled circle (rightmost symbol); a large open circle indicates that of CP Pup, which is due to N II 5005. Negative observations (no flux detected, upper limit about 10^{30} erg s^{-1}) are marked with the symbol "$\vee$".

The X-ray turnoff time of such objects is typically of the order one to several hundred days according to Vablandingham et al. (2001), so that the break in Hβ (and [O III]) around 1 year may have to do with the switching off of nuclear burning on the central object. At late stages (t of the order of 50 years), objects cluster at some 10^{30} ergs s^{-1}. No late Hβ observations exist for GK Per and CP Pup.

4.1.3 [O III]

Generally, [O III] λ5007 appears around age $\log t = -1.1$ (about a month after optical maximum), and remains within a factor 10 constant until $\log t = 0$ (i.e. one year after outburst). As in the case of Hβ, two well-expressed bands seem to be present, with the extragalactic novae populating the lower one. After two years, the [O III] λ5007 emission declines dramatically and for most objects is not recorded any more after 10 years. There are two noticeable exceptions: CP Pup and GK Per, which show emission at almost 10^{32} ergs s^{-1} 50 – 85 years after outburst. However, the luminosity from CP Pup is due to N II 5005, as was found spectroscopically by Williams (1982), while the emission in GK Per is indeed due to [O III] λ5007 (Bode et al. 1988).

The dichotomy that appeared in the Hβ luminosities is again clearly seen. A fit through the points with $\log t < 0$ yields

$$\begin{array}{rccc} \log(L_{5007}) = & 36.21 & - & 0.70 \log\ (\mathrm{age}) \\ & \pm 0.09 & & \pm 0.13 \end{array}$$

for the upper line, and

$$\begin{array}{rcccc} \log(L_{5007}) = & 34.97 & - & 0.94 \log\ (\mathrm{age}) \\ & \pm 0.14 & & \pm 0.22 \end{array}$$

for the lower one. Subsequently, both bands merge and a drop

$$\begin{array}{rcccc} \log(L_{5007}) = & 35.00 & - & 4.76 \log\ (\mathrm{age}) \\ & \pm 0.38 & & \pm 0.88 \end{array}$$

is observed. The last two data points, which belong to CP Pup and GK Per, were neglected in this fit. For the remaining novae, a luminosity of 10^{30} ergs s^{-1} is reached at $\log t = 1.05$, i.e. 11 years after outburst.

The maximum phase appears to reveal the presence of two groups, which show almost the same temporal behavior, but are clearly separated by a factor ~ 15 in emission line luminosity, with an amazingly low scatter. Among the objects in the bright group are V476 Cyg, GK Per, V603 Aql and V977 Sco; the faint group includes CP Lac, V1500 Cyg, V4157 Sgr, and V351 Pup. Interestingly, both groups contain the same mixture of Fe II/He-N novae, CO/ONeMg novae, so that there is no obvious parameter that influences the [O III] luminosity.

A clear outlier is V838 Her, whose [O III] λ5007 luminosity is about 100 times fainter than all other objects, except V4160 Sgr. The [O III] λ5007 lines emerge earlier than in any other object. A fit through the points of V838 Her yields:

$$\begin{array}{rcccc} \log(L_{5007}) = & 31.52 & - & 2.16 \log\ (\mathrm{age}). \\ & \pm 0.16 & & \pm 0.24 \end{array}$$

4.1.4 Additional remarks

The strong late emission of Hα and [O III] λ5007 in GK Per should be pointed out. GK Per is a peculiar nova shell which seems to interact with interstellar material or a fossil planetary nebula (Seaquist et al. 1989). Thus the ejected material shows shock interaction with the stationary circumstellar material, and remains in a hot state.

The noticeable emission in the [O III] λ5007 band of CP Pup is due to N II. CP Pup has, however, also an unusually strong Hα luminosity. Smits (1991) has argued for a small distance (between 525 and 850 pc) for CP Pup, which would lower the luminosity by factors 10 and 4, respectively. The intricate geometry (see Downes & Duerbeck (2000) for a detailed discussion) makes these values less likely, although they would bring the Hα luminosity closer to the average value found in other very fast novae of this age.

The peculiar case of V838 Her has already been mentioned. This was the nova with the shortest t_2 and t_3 times of the light curve decay. V838 Her appears to have less mass ejection, and thus a thin photosphere, which made the central object and its light changes appear after an unusually short time (Leibowitz et al. 1992). It is important to note that the poorly observed nova V4160 Sgr represents a second object of this rare class of rapidly fading neon novae with He-spectral characteristics. The three spectra available for V4160 Sgr (Williams 2000) resemble those of V838 Her (Vanlandingham et al. 1996) at similar phases.

4.2 Fast novae

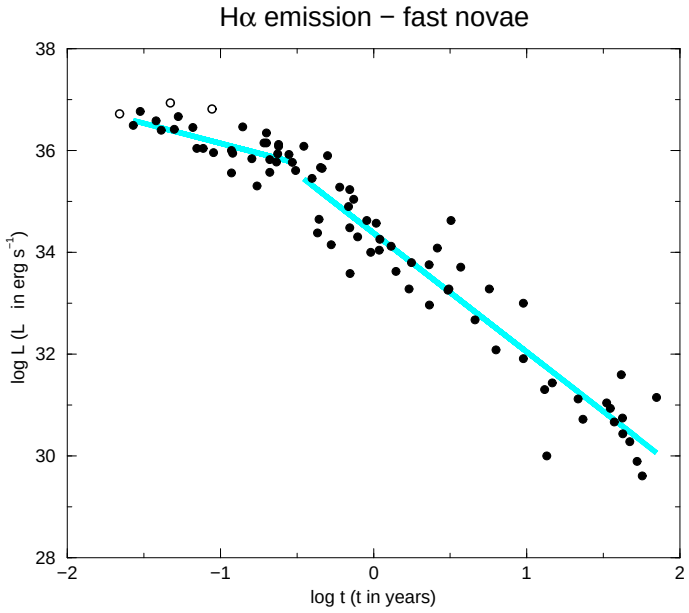

Figure 4: Hα luminosity versus time for fast novae. Galactic novae are shown as filled circles, extragalactic novae as open circles.

4.2.1 Hα

The trends in the evolution of line luminosities in the class of fast novae (Figs. 4 – 6) differ somewhat from those of very fast novae. The scatter between individual objects in this group is less pronounced. There is only one extragalactic nova (N LMC 1988-1) in the sample, which will be considered at the end.

Hα emission is first recorded at $\log t = -1.6$ (9 days after maximum), and slowly declines till $\log t = -0.5$ (115 days after maximum) by a factor 5. After that, a steeper decline sets in. At times $\log t < -0.5$ (115 days):

$$\begin{array}{rccc} \log(L_{\mathrm{H}\alpha}) = & 35.35 & - & 0.78 \log\ (\mathrm{age}), \\ & \pm 0.16 & & \pm 0.16 \end{array}$$

with an average value $\log(L_{\mathrm{H}\alpha}) = 36.08$, and at later times

$$\begin{array}{rccc} \log(L_{\mathrm{H}\alpha}) = & 34.38 & - & 2.34 \log\ (\mathrm{age}). \\ & \pm 0.10 & & \pm 0.11 \end{array}$$

4.2.2 Hβ

Hβ emission is first recorded at $\log t = -1.7$ (7 days after maximum), and slowly declines till $\log t = -0.5$ (115 days after maximum) by a factor 3. After that, a steeper decline sets in. The extragalactic nova lies noticeably above the other objects. If it would be placed among the very fast novae (and practically all other LMC novae are very fast novae), it would fit wery well into the corresponding diagrams. Such a case occurs from time to time: an object assigned to a group because of its light curve better fits into another group according to its

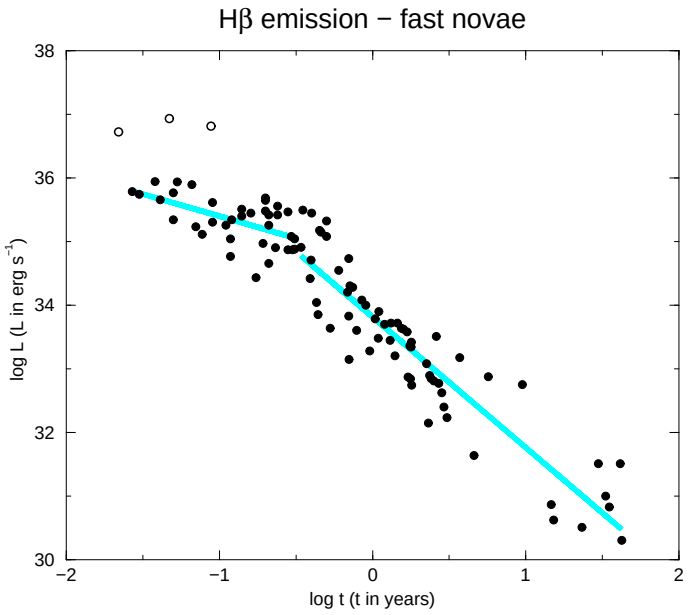

Figure 5: Hβ luminosity versus time for fast novae. Galactic novae are shown as filled circles, extragalactic novae as open circles.

line luminosity evolution. We will discuss the few cases in detail after the general discussion. At times $\log t < -0.5$ (115 days):

$$\log(L_{\mathrm{H}\beta}) = \underset{\pm 0.16}{34.70} - \underset{\pm 0.17}{0.69} \log\ (\mathrm{age}),$$

with an average value $\log(L_{\mathrm{H}\beta}) = 35.32 \pm 0.38$ ergs s^{-1}, and at later times

$$\log(L_{\mathrm{H}\beta}) = \underset{\pm 0.07}{33.81} - \underset{\pm 0.11}{2.05} \log\ (\mathrm{age}).$$

4.2.3 [O III]

In fast novae, [O III] λ5007 shows up at $\log t = -0.9$ (46 days after maximum). It displays a continuous decline in strength (a factor of about 50) until a breakpoint that can only be approximately determined because of the large scatter. The breakpoint can be put at $\log t = 0$ as well as at $\log t = 0.5$, i.e. 1 to 3.2 years after outburst. We will assume $\log t = 0.25$ as the position of the breakpoint. After that, a steeper decline sets in.

At early stages $-1 < \log t < 0.25$, the average $\log(L_{5007}) = 34.95 \pm 0.53$ ergs s^{-1}, a fit through these points with yields

$$\log(L_{5007}) = \underset{\pm 0.09}{34.68} - \underset{\pm 0.21}{0.98} \log\ (\mathrm{age}).$$

Subsequently, a drop

$$\log(L_{5007}) = \underset{\pm 0.26}{35.60} - \underset{\pm 0.44}{3.73} \log\ (\mathrm{age})$$

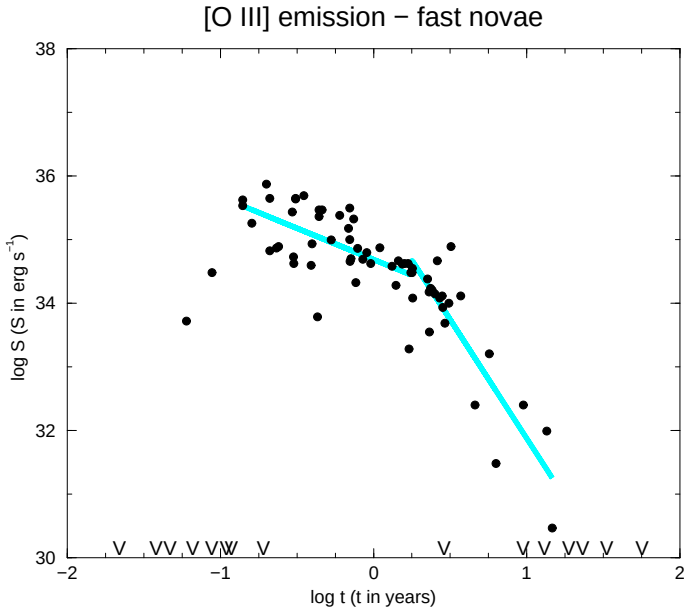

Figure 6: [O III] λ5007 luminosity versus time for fast novae. Galactic novae are shown as filled circles, extragalactic novae as open circles. Negative observations (no flux detected, upper limit about 10^{30} erg s^{-1}) are marked with the symbol "$\vee$".

is observed. This means that, on the average, a luminosity of 10^{30} ergs s^{-1} is reached at $\log t = 1.50$, i.e. 32 years after outburst.

4.2.4 Additional remarks

The X-ray turnoff time of ONeMg novae of the fast speed class like QU Vul and V1974 Cyg is of the order $1.5 - 4$ years according to Vanlandingham et al. (2001). This might coincide with the time when the [O III] λ5007 emission starts to fade noticeably.

4.3 Moderately fast novae

4.3.1 Hα

Some moderately fast novae have been caught in very early stages, with fairly strong or weak Hα emission lines, but the sample is too small to draw any conclusions. Between $\log t = -1.5$ and -0.5 (12 days and 115 days), a fairly well-expressed maximum is reached. Afterwards, a decline with a slope of ~ -2 sets in. At times $\log t < -0.5$,

$$\begin{array}{rcccc} \log(L_{\mathrm{H}\alpha}) = & 35.68 & - & 0.08\log\ (\mathrm{age}), \\ & \pm 0.27 & & \pm 0.28 \end{array}$$

with an average value $\log(L_{\mathrm{H}\alpha}) = 35.8 \pm 0.5$ erg s^{-1}, and at later times

$$\begin{array}{rcccc} \log(L_{\mathrm{H}\alpha}) = & 34.26 & - & 2.06\log\ (\mathrm{age}). \\ & \pm 0.15 & & \pm 0.15 \end{array}$$

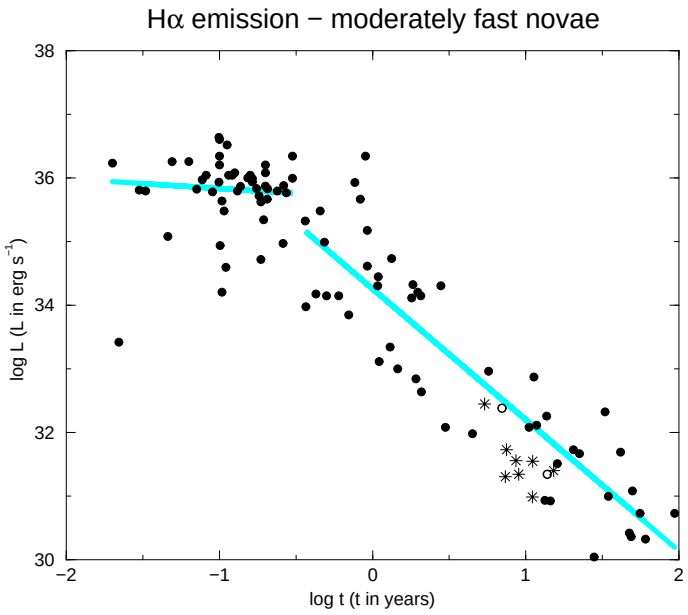

Figure 7: Hα luminosity versus time for moderately fast novae. Galactic novae are shown as filled circles. The "slow" nova PW Vul is shown with open circles; it fits very well into the general trend. The peculiar nova GQ Mus is shown with asterisks.

Figures 7 – 9 show two objects with special symbols. Open circles denote data for the slow nova PW Vul, which fits quite well into the group of moderately fast novae. Asterisks denote fluxes of the peculiar nova GQ Mus.

4.3.2 Hβ

As in the case of Hα, in Hβ the time between $\log t = -1.5$ and -0.5 (12 days and 115 days) is marked by a large scatter, but no obvious general decline is noticeable. Afterwards, the decline in luminosity is obvious, however also marked by large scatter. The slope after 4 months is -1.78, slightly shallower than for fast and very fast novae.

At times between $\log t = -1.5$ and $\log t = -0.5$,

$$\begin{array}{rcccc} \log(L_{\mathrm{H}\beta}) = & 34.71 & - & 0.18 \log\ (\mathrm{age}), \\ & \pm 0.26 & & \pm 0.27 \end{array}$$

with an average value $\log(L_{\mathrm{H}\beta}) = 34.88 \pm 0.68$ ergs s^{-1}, and at later times

$$\begin{array}{rcccc} \log(L_{\mathrm{H}\beta}) = & 33.61 & - & 1.88 \log\ (\mathrm{age}). \\ & \pm 0.11 & & \pm 0.15 \end{array}$$

Again, the luminosities of the slow nova PW Vul emulate those of moderately fast novae, while the peculiar X-ray active nova GQ Mus shows a much more rapid decline than other novae.

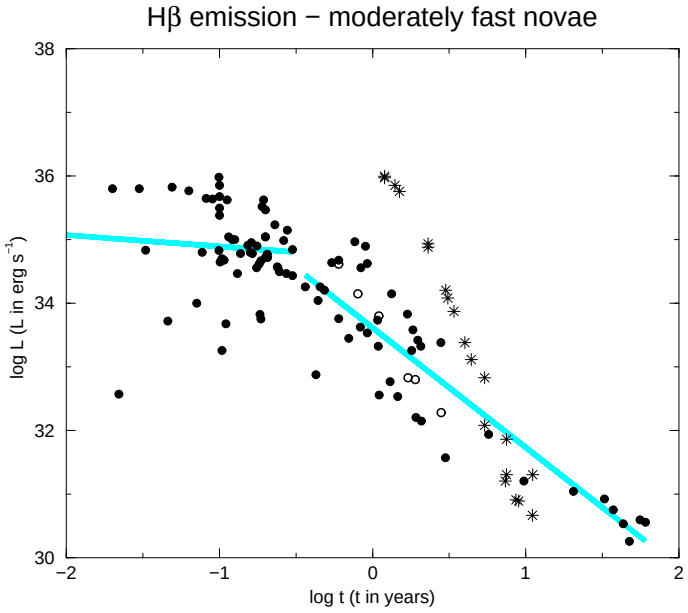

Figure 8: Hβ luminosity versus time for moderately fast novae. Galactic novae are shown as filled circles. The "slow" nova PW Vul is shown with open circles; it fits very well into the general trend. The peculiar nova GQ Mus is shown with asterisks.

4.3.3 [O III]

For moderately fast novae, the [O III] λ5007 data are somewhat sparse. [O III] λ5007 shows up after $\log t = -0.4$ (145 days), and persists with fairly constant strength until $\log t = 0.4$ (2.5 years). Afterwards, a quite dramatic decline sets in.

Between $-0.4 < \log t < 0.4$, the average $\log(L_{5007}) = 35.39 \pm 0.63$ erg s^{-1}, while a fit through the points with $\log t > 0.4$, excluding the novae GQ Mus and PW Vul and the late value of DQ Her, yields

$$\log(L_{5007}) = \underset{\pm 0.79}{36.73} - \underset{\pm 0.80}{4.86} \log\ (\text{age}).$$

On the average, a luminosity of 10^{30} ergs s^{-1} is reached at $\log t = 1.38$, i.e. 24 years after outburst.

4.3.4 Additional remarks

The similarity of the evolution of the slow nova PW Vul with the majority of moderately fast novae has already been pointed out. It is also interesting to note that the decline in [O III] λ5007 is very similar in fast and moderately fast novae (although [O III] λ5007 appears much earlier in fast novae).

An important point is the unusually bright [O III] λ5007 luminosity determined for DQ Her 50 years after outburst. The [O III] λ5007 filter exposure has certainly picked up emission of the line N II 5005, which was observed spectroscopically by Williams et al. (1978) at the endpoints of the major axis of the shell. Indeed, the direct image of 1984 shows a deficit of emission along the minor axis.

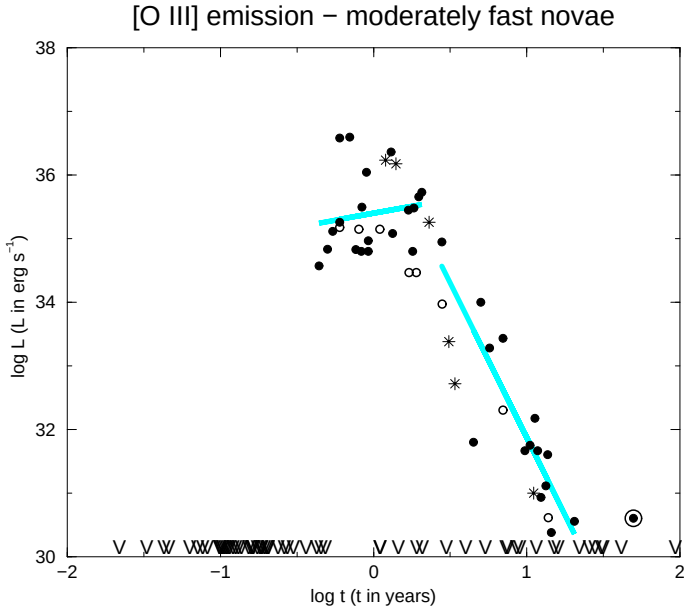

Figure 9: [O III] λ5007 luminosity versus time for moderately fast novae. Galactic novae are shown as filled circles. The "slow" nova PW Vul is shown with open circles; it fits very well into the general trend. The peculiar nova GQ Mus is shown with asterisks. The flux in the shell of DQ Her at late stages is due to N II 5005 (encircled filled circle). Negative observations (no flux detected, upper limit about 10^{30} erg s^{-1}) are marked with the symbol "$\vee$".

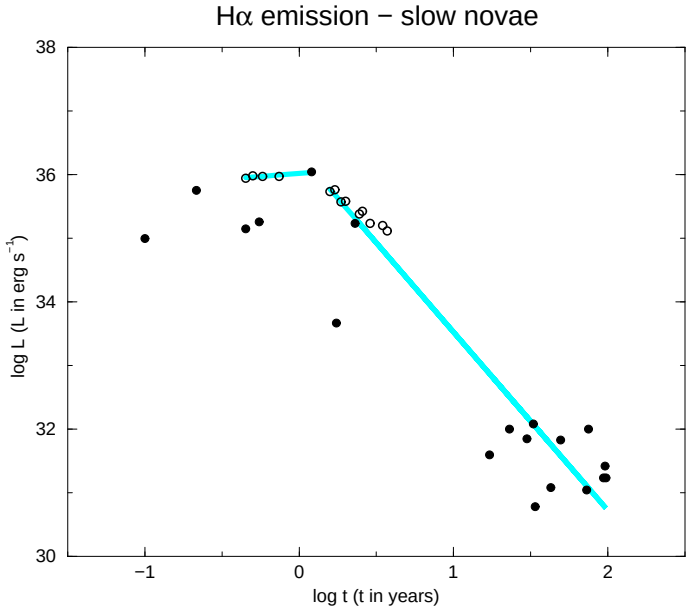

Figure 10: Hα luminosity versus time for slow novae. Galactic novae are shown as filled circles, extragalactic novae as open circles.

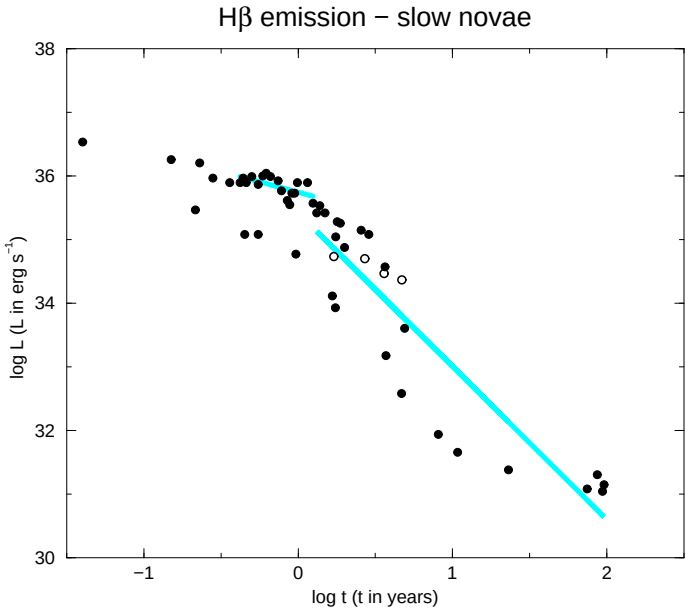

Figure 11: Hβ luminosity versus time for slow novae. Galactic novae are shown as filled circles, extragalactic novae as open circles.

4.4 Slow and very slow novae

4.4.1 Hα

Flux data are only available for a handful of novae, making general statements quite uncertain. The main string of data (see Figs. 10 – 12), is from M31-C32, a well-monitored extragalactic very slow nova. A few data points from V723 Cas fall remarkably close to this object. Thus it seems that the luminosity discrepancy between novae in M31 and the Galaxy occurs only among very fast novae.

Note that some novae, like RR Pic, HR Del and V723 Cas have an extended pre-maximum halt. Because of the logarithmic plot, emission line fluxes are plotted only after maximum light. The number of studied objects is somewhat scarce, and the behavior of slow novae is quite varying, so these fits are not as representative as those for the other speed classes.

The luminosity remains essentially constant between $\log t = -0.4$ and $\log t = 0.1$ (145 – 460 days after maximum), and declines afterwards.

At times $-0.4 < \log t < +0.1$,

$$\begin{array}{rccc} \log(L_{\mathrm{H}\alpha}) = & 36.02 & + & 0.19 \log\ (\mathrm{age}) \\ & \pm 0.01 & & \pm 0.06 \end{array}$$

with an average value $\log(L_{\mathrm{H}\alpha}) = 35.98 \pm 0.04$ erg s^{-1}, and at later times

$$\begin{array}{rccc} \log(L_{\mathrm{H}\alpha}) = & 36.33 & - & 2.80 \log\ (\mathrm{age}) \\ & \pm 0.22 & & \pm 0.18 \end{array}$$

Hα emission from the shell is still observed in very old remnants.

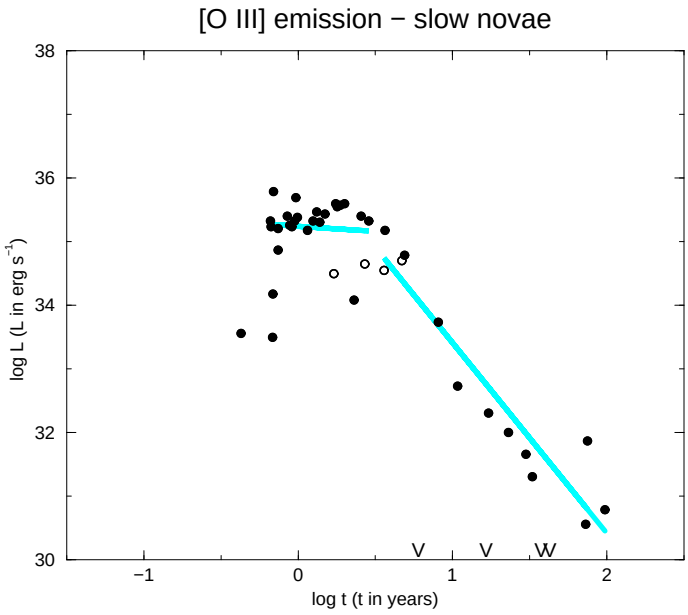

Figure 12: [O III] λ5007 luminosity versus time for slow novae. Galactic novae are shown as filled circles, extragalactic novae as open circles. Negative observations (no flux detected, upper limit about 10^{30} erg s^{-1}) are marked with the symbol "$\vee$".

4.4.2 Hβ

Here we have a long data series of RR Pic, from the presumable maximum onward, plus data from HR Del and V868 Cen. Between $\log t = -2$ and $\log t = 0.1$ (3 days – 460 days after maximum), the behavior of the Hβ flux declines very slowly by a factor 4. After 460 days, the slope becomes steeper.

At times $-0.4 < \log t < +0.1$,

$$\begin{array}{rcccc} \log(L_{\mathrm{H}\beta}) = & 35.74 & - & 0.65 \log\ (\mathrm{age}), \\ & \pm 0.04 & & \pm 0.22 \end{array}$$

with an average value $\log(L_{\mathrm{H}\beta}) = 35.84 \pm 0.16$ erg s^{-1}, and at later times

$$\begin{array}{rcccc} \log(L_{\mathrm{H}\beta}) = & 35.42 & - & 2.41 \log\ (\mathrm{age}). \\ & \pm 0.21 & & \pm 0.22 \end{array}$$

Hβ emission from the shell is still observed in very old remnants.

4.4.3 [O III]

In slow novae, [O III] λ5007 emission appears at time $\log t = -0.2$, about 230 days after maximum. RR Pic and HR Del show almost constant [O III] λ5007 flux between the first appearance at 0.6 years up to $\log t = 0.5$, 3 years after maximum.

The average $\log(L_{5007}) = 35.22 \pm 0.43$ erg s^{-1}, a fit through the points with $\log t < 0.5$ yields

$$\begin{array}{rcccc} \log(L_{5007}) = & 35.24 & - & 0.16 \log\ (\mathrm{age}). \\ & \pm 0.09 & & \pm 0.43 \end{array}$$

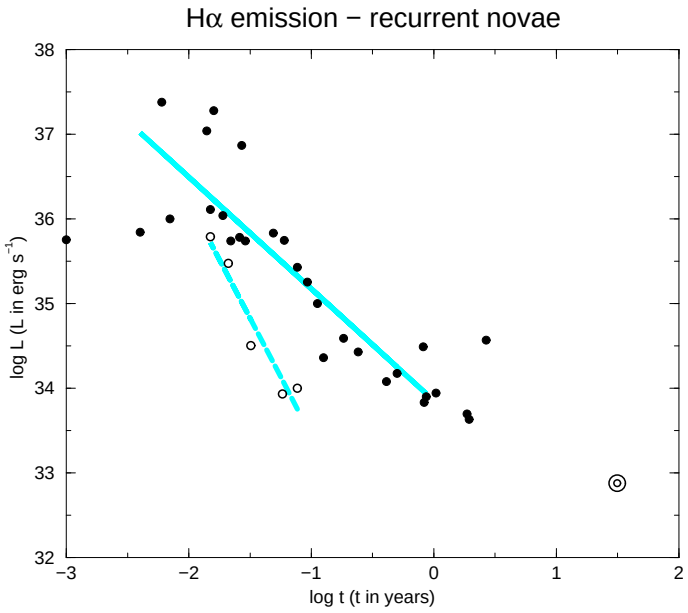

Figure 13: Hα luminosity versus time for recurrent novae. Galactic objects with giant companions are shown as filled circles, galactic objects with dwarf companions as open circles. The recent flux of the slow recurrent nova T Pyx is shown as an encircled open circle.

In the following century, a drop

$$\begin{array}{rccc} \log(L_{5007}) = & 36.40 & - & 3.00 \log\ (\text{age}) \\ & \pm 0.38 & & \pm 0.29 \end{array}$$

is observed.

Note that the decline from maximum is documented only by data of HR Del. A few very old remnants, RR Pic, DO Aql and X Ser still show [O III] λ5007 emission, which is, in two cases, documented by spectroscopy (and thus confusion with N II, as in CP Pup and DQ Her, can be ruled out). Such a behavior is at variance with all other types of classical novae, and indicates that a source of high energy photons, presumably from the nuclear burning in the outer layers of the white dwarf, is still active $\sim$ 100 years after outburst.

4.4.4 Additional Remarks

Most notable are the [O III] λ5007-bright shells around old slow novae.

4.5 Recurrent Novae

At least three distinct groups of recurrent novae can be discriminated: very fast novae with dwarf companions, very fast novae with giant companions, and the slow recurrent nova T Pyx. The most extensive data set exists for the second group, and it is obvious that the other groups behave differently: the fast recurrent novae with dwarf secondaries show an extremely rapid decline of emission line strength in the Balmer lines, and [O III] λ5007 is basically absent (see Figs. 13 – 15). The slow recurrent nova T Pyx shows, more than thirty

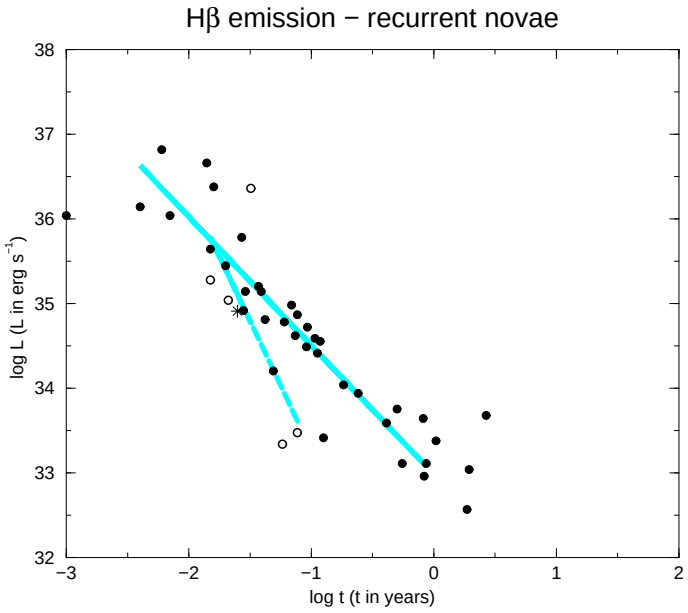

Figure 14: Hβ luminosity versus time for recurrent novae. Galactic objects with giant companions are shown as filled circles, galactic objects with dwarf companions as open circles; the extragalactic recurrent nova LMC 1988-2, which also has a dwarf companion, is shown with an asterisk.

years after its most recent outburst, persistently strong Hα and [O III] λ5007 emission, likely because of shock interaction of ejecta from different outbursts.

4.5.1 Hα

In the interval $-2.5 < \log t < 0$, recurrent novae with giant companions have

$$\log(L_{\mathrm{H}\alpha}) = \underset{\pm 0.22}{33.85} - \underset{\pm 0.15}{1.32} \log\ (\mathrm{age}).$$

Recurrent novae with dwarf companions show a more rapid decrease in flux:

$$\log(L_{\mathrm{H}\alpha}) = \underset{\pm 0.67}{30.67} - \underset{\pm 0.45}{2.77} \log\ (\mathrm{age}).$$

4.5.2 Hβ

At times $-2.5 < \log t < 0$, recurrent novae with giant companions show

$$\log(L_{\mathrm{H}\beta}) = \underset{\pm 0.14}{32.99} - \underset{\pm 0.11}{1.52} \log\ (\mathrm{age}).$$

Recurrent novae with dwarf companions show a more rapid decrease in flux:

$$\log(L_{\mathrm{H}\beta}) = \underset{\pm 2.63}{30.22} - \underset{\pm 1.77}{3.05} \log\ (\mathrm{age}).$$

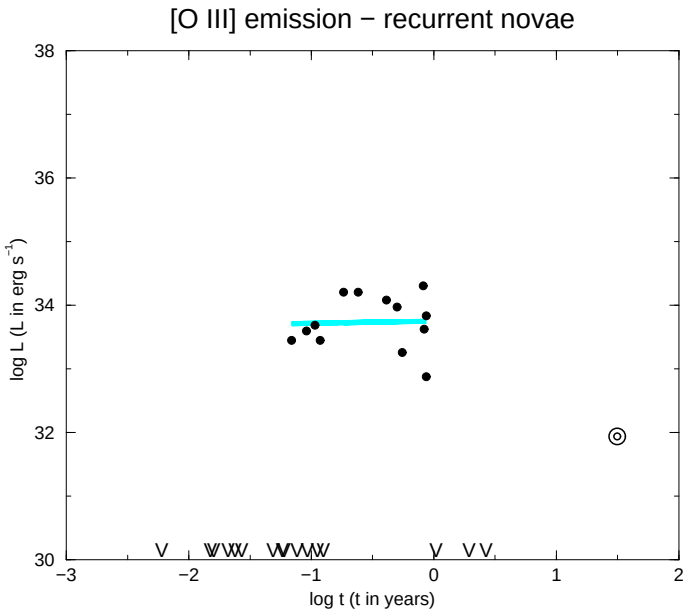

Figure 15: [O III] λ5007 luminosity versus time for recurrent novae. Galactic objects with giant companions are shown as filled circles. Galactic objects with dwarf companions seem to show no [O III] emission; the only exception is the slow recurrent nova T Pyx, whose recent flux is shown as an encircled open circle. Negative observations (no flux detected, upper limit about 10^{30} erg s^{-1}) are marked with the symbol "$\vee$".

4.5.3 [O III]

No [O III] λ5007 flux measurements in recurrent novae with dwarf companions are known; these features are either very weak or do not appear. Early weak [O III] λ5007 emission, caused by photoionization of the giant wind by the energetic radiation from the early outburst, has been reported for V745 Sco.

Noticeable emission in [O III] λ5007 starts to appear at $\log t = -1.2$, reaches a maximum at $\log t = -0.5$, and declines afterwards. A fit is uncertain for lack of secure data, but the average flux at times before one year is $\log(L_{5007}) = 33.73 \pm 0.42$ erg s^{-1}. T Pyx is still bright in [O III] λ5007 30 years after the last outburst: Interaction with previous shells keeps the ejecta hot, which appears to be untypical for other, faster recurrent novae. Thus we refrain from merging data of very different objects, as we have also considered RN with dwarf and giant companions separately.

5 Summary

We have collected about 1200 available line fluxes of 96 classical and recurrent novae of various speed classes and have studied the evolution of the luminosity in the Hα, Hβ, and [O III] λ5007 line as a function of time after outburst. In general, novae of a given speed class follow similar patterns, so that functional relations for the average evolution of line luminosity could be derived. General trends for novae of various speed classes are shown in Figs. 15, 16 and 17. A few novae turn out to be unusual: GK Per and T Pyx, which

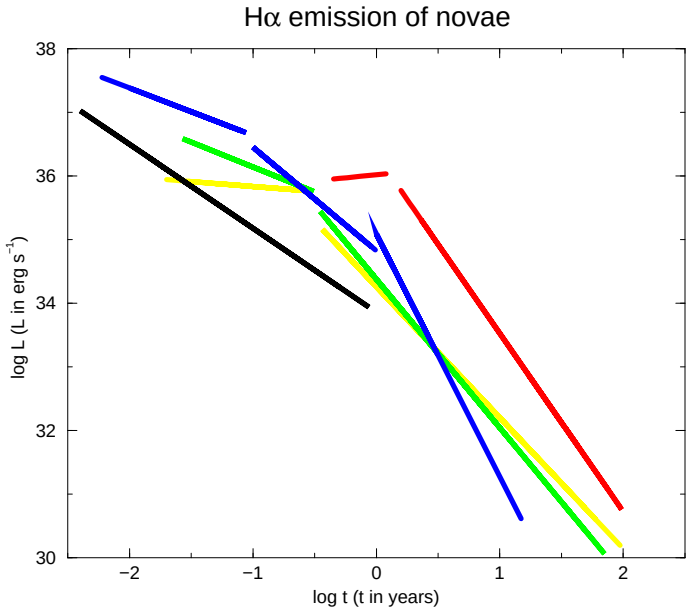

Figure 16: Averaged time dependence of Hα emission in novae of various speed classes: very fast (blue), fast (green), moderately fast (yellow), slow and very slow (red), and recurrent novae with giant companions (black). At late times, decay occurs fastest in very fast novae, somewhat more slowly in slow novae, and slowest in fast and moderately fast novae. Contrary to the behaviour in classical novae, the decay of Hα emission in recurrent novae sets in immediately after maximum, and continues without any break in slope.

interact with circumstellar material, V838 Her and V4160 Sgr, which have unusually small mass ejection, and GQ Mus, an X-ray emitting classical nova.

A general discussion of the material presented here in the framework of nova properties and shell evolution will be presented elsewhere (Duerbeck & Downes 2002). The data of Tables 1 – 4 are also included as ascii files in `table1.dat, table2.dat, table3.dat` and `table4.dat`.

6 Appendix: Notes on some nova distances

DO Aql - This is a very interesting slow nova; unfortunately the light curve has a large seasonal gap, and the true maximum may have been missed. The reddening is low even for large distances, $A_V = 0.41$. Application of the MMRD yields a distance $d = 9.5$ kpc; if DO Aql has a luminosity that is similar to the faintest nova in the MMRD sample, a minimum distance $d = 3.6$ kpc follows. A distance $d = 6.5 \pm 3.0$ is plausible.

V365 Car - The light curve and its parameters (Liller & Henize 1975) indicate a slow nova for which an average absolute magnitude $M_V = -7.09$ is assumed. Since the light curve is photographic, a $(B - V)$ correction of 0.25 was applied. The galactic extinction program (Hakkila et al. 1997) yields an $A_V = 2.7$ for a distance of 4.7 kpc, which yields the expected apparent magnitude.

V868 Cen - The nova until now had a poor light curve coverage. There were also discrepant reports on dust formation (Smith et al. 1995; Harrison et al. 1998). The photo-

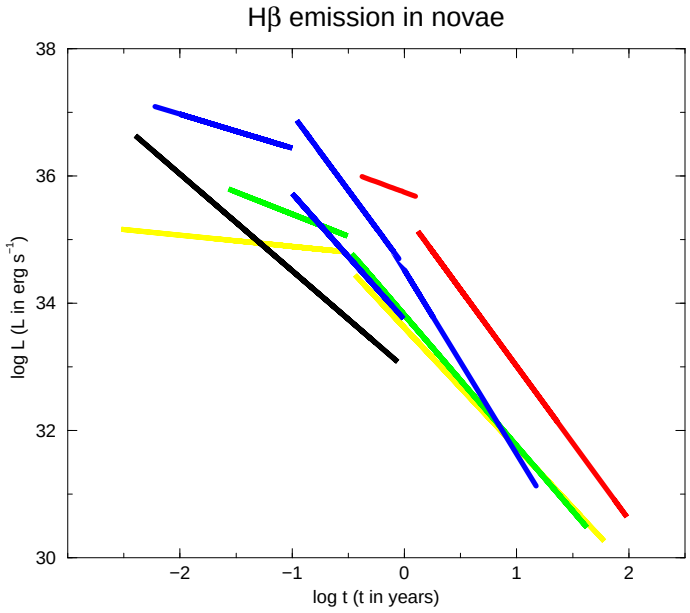

Figure 17: Averaged time dependence of Hβ emission in novae of various speed classes: very fast (blue), fast (green), moderately fast (yellow), slow and very slow (red), and recurrent novae with giant companions (black). Note that the behaviour of Hβ in novae of different speed classes is quite similar to that shown in Hα. Contrary to the behaviour in classical novae, the decay of Hβ emission in recurrent novae sets in immediately after maximum, and continues without any break in slope.

metric observations published in the IAU Circulars were supplemented by an extended series of visual estimates (Jones 2001). They lead us: (1) to reclassify V868 Cen as a medium fast nova, (2) to time the dust formation at the epoch of the IR observations of Harrison et al. (1998) (but certainly later than the IR spectroscopy of Smith et al. (1995), which however, did not develop into a dramatic visual minimum, but a short depression, similar to those observed in NQ Vul), and (3) to derive a consistent distance and reddening.

V888 Cen - Light curve data were taken from the IAU Circulars, and $m \approx 7$, $t_3 = 20$ days was estimated. Using the MMRD, a consistent distance and reddening ($d = 5100$ pc, $A_V = 2.65$) was found.

BY Cir - Light curve data were taken from the IAU Circulars, and $m \approx 7$, $t_2 = 11$ days was estimated. Using the MMRD, a consistent distance and reddening ($d = 6000$ pc, $A_V = 2.31$) was found.

V2295 Oph - Light curve data were taken from the IAU Circulars, and $m \approx 9.3$, was estimated. The light curve seems to indicate a plateau, followed by dust formation, and a light curve type C was assumed, which is typical for novae with $M_V \sim 7.09$. A consistent distance and reddening ($d = 10$ kpc, $A_V = 1.27$) was found.

V4361 Sgr - Light curve data were taken from the IAU Circulars, and $m \approx 10.5$, was estimated. The nova curve is fragmentary, but the nova appears to evolve slowly, thus $M_V = -7.09$ was assumed. A consistent distance and reddening ($d = 4600$ pc, $A_V = 4.34$) was found.

V4633 Sgr - Light curve data were taken from Liller & Jones (1999), and $m \approx 7.8$, $t_3 = 52$ days was estimated. Using the MMRD, an $M_V = -7.75$ was estimated, and a

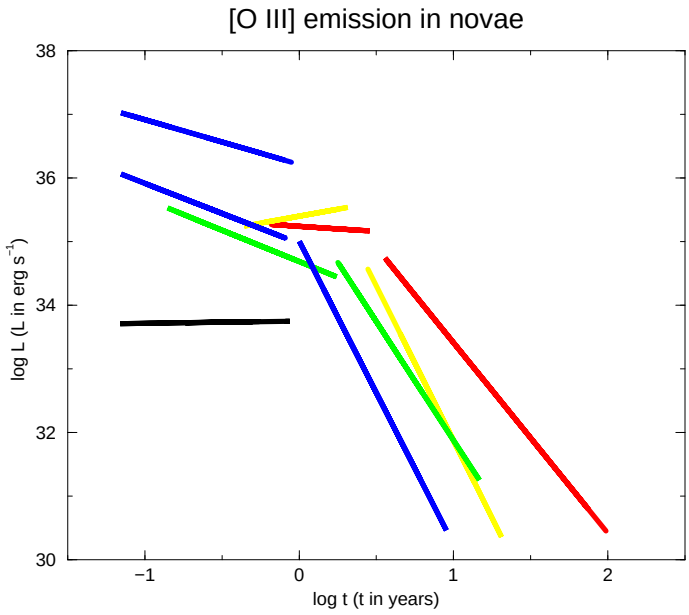

Figure 18: Averaged time dependence of [O III] λ5007 emission in novae of various speed classes: very fast (blue), fast (green), moderately fast (yellow), slow and very slow (red), and recurrent novae with giant companions (black). At late times, decay occurs fastest in very fast novae, almost as fast in moderately fast and fast novae, and slowest in slow novae, i.e. shells of slow novae show noticeable [O III] λ5007 emission also at late times. [O III] λ5007 emission in recurrent novae appears to be "on" for some time and afterwards disappears quickly.

consistent distance and reddening ($d = 7300$ pc, $A_V = 1.23$) was found.

V4642 Sgr - Light curve data were taken from the IAU Circulars. The very fragmentary light curve indicates a nova which is not fast; maximum $m \approx 10$. The absolute magnitude was assumed as $M = -7$. A consistent distance and reddening ($d = 6700$ pc, $A_V = 2.72$) was found.

V1141 Sco - Light curve data were taken from the IAU Circulars. The light curve indicates a very fast nova with $t_2 \approx 3^d, t_3 \approx 7^d$, The MMRD yields an absolute magnitude of $M = -9.8$. A consistent distance and reddening ($d = 7300$ pc, $A_V = 3.98$) was found.

V1142 Sco - Light curve data were taken from Liller & Jones (1999). The light curve indicates a very fast nova with $t_2 \approx 8^d, t_3 \approx 12 - 22^d$, maximum light was assumed to be $m_v = 7$. The MMRD yields an absolute magnitude of $M = -9.25$. A consistent distance and reddening ($d = 6100$ pc, $A_V = 2.32$) was found.

Acknowledgments

We thank Bob Williams (STScI) for providing the data for the Tololo Nova Survey objects, and Albert Jones for providing his series of visual observations of V868 Cen. We also thank the referee, A. Jorissen, for his comments. This research has made use of NASA's Astrophysics Data System Bibliographic Services, as well as of the SIMBAD database, operated at CDS, Strasbourg, France. This project was supported by the Flemish Ministry for Foreign

Policy, European Affairs, Science and Technology.

References

Acker, A., Marcout, J., Ochsenbein, F., Stenholm, B., and Tylenda, R. 1992, Strasbourg-ESO Catalogue of Galactic Planetary Nebulae (ESO, Germany)

Anderson, C.M. and Gallagher, J.S. 1977, PASP, 89, 264

Andreä, J., Drechsel, H., and Starrfield, S. 1994, A&A, 291, 869

Anupama, G.C., Duerbeck, H.W., Prabhu, T.P., and Jain, S.K. 1992, A&A, 263, 87

Anupama, G.C. and Dewangan, G.C. 2000, AJ, 119, 1359

Anupama, G.C. and Sethi, S. 1994, MNRAS, 269, 105

Bahng, J.D.R., 1972, MNRAS, 158, 151

Bertaud, C. 1948, Annales d'Astrophysique, 11, 1

Bode, M.F., Duerbeck, H.W., Seitter, W.C., Albinson, J.S., and Evans, A. 1988, in A Decade of UV Astronomy with the IUE Satellite, ESA-SP 281, Vol. 1, 183

Bohigas, J., Echevarría, J., Diego, F., and Sarmiento, J.A. 1989, MNRAS, 238, 1395

Ciardullo, R., Ford, H.C., Neill, J.D., Jacoby, G.H., and Shafter, A.W. 1987, ApJ, 318, 520

Ciardullo, R., Shafter, A.W., Ford, H.C., Neill, J.D., Shara, M.M. and Tomaney, A.B. 1990, ApJ, 356, 472

Ciatti, F. and Rosino, L. 1974, A&AS, 16, 305

Copetti, M.V.S. 1990, PASP, 102, 77

de Freitas Pacheco, J.A., Da Costa, R.D.D., and Codina, S.J. 1989, ApJ, 347, 483

Della Valle, M. 1991, A&A, 252, L9

Della Valle, M. and Duerbeck, H.W. 1993, A&A, 275, 239

Della Valle, M., Gilmozzi, R., Bianchini, A., and Esenoglu, H. 1997, A&A, 325, 1151

Della Valle, M. and Livio, M. 1998, ApJ, 506, 818

Diaz, M.P., Williams, R.E., Phillips, M.M., and Hamuy, M. 1995, MNRAS, 277, 959

Dopita, M.A., and Hua, C.T. 1997, ApJS, 108, 515

Downes, R.A. and Duerbeck, H.W. 2000, AJ, 120, 2007 Institute, Erlangen-Nuremberg University.

Duerbeck, H.W., and Downes, R.A. 2002, in preparation

Ferland, G.J., Lambert, D.L., and Woodman, J.H. 1986, ApJS, 60, 375

Ferland, G.J., Williams, R.E., Lambert, D.L., Slovak, M., Gondhalekar, P.M., Truran, J. W., and Shields, G. A. 1984, ApJ, 281, 194

Gehrz, R.D., Jones, T.J., Woodward, C.E., Greenhouse, M.A., Wagner, R.M., Harrison, T.E., Hayward, T.L., and Benson, J. 1992, ApJ, 400, 671

Gilmozzi, R., Selvelli, P., and Cassatella, A. 1998, Ultraviolet Astrophysics beyond the IUE final archive, ESA SP-413, eds. W. Wamsteker and R. González Riestra, p. 415

González-Riestra, R. 1992, A&A, 265, 71

Hachisu, I. and Kato, M. 2000a, ApJ, 540, 447

Hachisu, I. and Kato, M. 2000b, ApJ, 536, L93

Hachisu, I., Kato, M., Kato, T., Matsumoto, K. 2000, ApJ, 234, L189

Hakkila, J., Myers, J.M., Stidham, B.J., and Hartmann, D.H. 1997, AJ, 114, 2043

Hang, H., Zhu, Z., and Liu, Q. 1999, Acta Astron. Sinica 40, 247

Harrison, T.E., Johnson, J.J., Mason, P.A., and Stringfellow, G.S. 1998, in ASP Conf. 137, Wild Stars in the Old West, ed. S. Howell, E. Kuulkers, and Chick Woodward (San Francisco: ASP), 489

Hauschildt, P.H., Starrfield, S., Shore, S.N., Gonźalez-Riestra, R., Sonneborn, G., and Allard, F. 1994, AJ, 108, 1008

Honeycutt, R.K., Robertson, J.W., and Turner, G.W. 1995, ApJ, 446, 838

Jones, A. 2001, private communication

Kalużny, J. and Chlebowski, T. 1988, ApJ, 332, 287

Kamath, U.S., Anupama, G.C., Ashok, N.M., and Chandrasekhar, T. 1997, AJ, 114, 2671

Kawabata, K.S., Hirata, R., Ikeda, Y., Akitaya, H., Seki, M., Matsumura, M., and Okazaki, A. 2000, ApJ, 540, 429

Larsson-Leander, G. 1954, Stockholm Obs. Ann. 18, No. 4

Leibowitz, E.M., Mendelson, H., Mashal, E., Prialnik, D., and Seitter, W.C. 1992, ApJ, 385, L49

Liller, W. and Henize, K.G. 1975, ApJ, 200, 694

Liller, W. and Jones, A. 1999, IBVS, 4664

Liu, W., and Hu, J.Y. 2000, ApJS, 128, 387

Lynch, D.K., Rossano, G.S., Rudy, R.J., and Puetter, R.C. 1995, AJ, 110, 227

Lynch, D.K., Rudy, R.J., Rossano, G.S., Erwin, P., and Puetter, R.C. 1989, AJ, 98, 1682

Matheson, T., Filippenko, A.V., and Ho, L.C. 1993, ApJ, 418, L29

McLaughlin, D.B. 1939, Pop. Astr., 47, 410, 481, 538

McLaughlin, D.B. 1944, AJ, 51, 20

McLaughlin, D.B. 1953, ApJ, 117, 279

Morisset, C. and Péquignot, D. 1996, A&A, 312, 135

Munari, U., Goranskij, V.P., Popova, A.A. et al. 1996, A&A, 315, 166

Munari, U., Yudin, B.F., Kolotilov, E.A., Shenavrin, V.I., Sostero, G., and Lepardo, A. 1994, A&A, 284, L9

Mustel, E.R. and Boyarchuk, A.A. 1970, Ap&SS, 6, 183

Payne-Gaposchkin, C. 1957, The Galactic Novae (Interscience Publishers, Inc.: New York)

Payne-Gaposchkin, C. and Menzel, D.H. 1938, Harvard College Circ. 428

Payne-Gaposchkin, C. and Gaposchkin, S. 1942, Harvard College Circ. 445

Péquignot, D., Petitjean, P., Boisson, C., and Krautter, J. 1993, A&A, 271, 219

Perinotto, M., Purgathofer, A., Pasquali, A., and Patriarchi, P. 1994, A&AS, 107, 481

Popper, D.M. 1940, ApJ, 92, 262

Rafanelli, P. Rosino, L., and Radovich, M. 1995, A&A, 294, 488

Retter, A., Leibowitz, E.M., and Naylor, T. 1999, MNRAS, 308, 140

Ringwald, F.A. Naylor, T. and Mukai, K. 1996, MNRAS, 281, 192

Rosino, L., Iijima, T., Benetti, S., D'Ambrosio, V., Di Paolantonio, A., and Kolotilov, E.E. 1992, A&A, 257, 603

Saizar, P., Pachoulakis, I., Shore, S.N., Starrfield, S., Williams, R.E., Rothschild, E., and Sonneborn, G., 1996, MNRAS, 279, 280

Saizar, P., Starrfield, S., Ferland, G.J., Wagner, R.M., Truran, J.W., Kenyon, S. J., Sparks, W. M., Williams, R. E., and Stryker, L. L. 1991, ApJ, 367, 310

Saizar, P., Starrfield, S., Ferland, G.J., Wagner, R.M., Truran, J.W., Kenyon, S.J., Sparks, W.M., Williams, R.E., and Stryker, L.L. 1992, ApJ, 398, 651

Schwarz, G.J., Hauschildt, P.H., Starrfield, S., Baron, E., Allard, F., Shore, S.N., and Sonneborn, G. 1997, MNRAS, 284, 669

Scott, A.D., Evans, A., and Rawlings, J.J.M. 1994, MNRAS, 269, L21

Scott, A.D., Duerbeck, H.W., Evans, A., Chen, A.-L., de Martino, D., Hjellming, R., Krautter, J., Laney, D., Parker, Q.A., Rawlings, J.M.C., and Van Winckel, H. 1995, A&A, 296, 439

Seaquist, E.R., Bode, M.F., Frail, D.A., Roberts, J.A., Evans, A., and Albinson, J.S. 1989, ApJ, 344, 805

Sekiguchi, K., Whitelock, P.A., Feast, M.W., Barrett, P.E., Caldwell, J.A.R., Carter, B.S., Catchpole, R.M., Laing, J.D., Laney, C.D., Marang, F., and van Wyk, F. 1990a, MNRAS, 246, 78

Sekiguchi, K., Stobie, R.S., Buckley, D.A.H., and Caldwell, J.A.R. 1990b, MNRAS, 245, 28p

Shafter, A.W. 1997, ApJ, 487, 226

Shaw, R.A. and Kaler, J.B. 1989, ApJS, 69, 495

Shore, S.N. Sonneborn, George; Starrfield, Sumner G.; Hamuy, M.; Williams, R. E.; Cassatella, A.; Drechsel, H.et al. 1991, ApJ, 370, 193

Smits, D.P. 1991, MNRAS, 248, 217

Smith, C.H., Aitken, D.K., Roche, P.F., and Wright, C.M. 1995, MNRAS, 277, 259

Snijders, M.A.J., Batt, T.J., Seaton, M.J., Blades, J.C., and Morton, D.C. 1984, MNRAS, 211, 7p

Snijders, M.A.J., Batt, T.J., Roche, P.F., Seaton, M.J., Morton, D.C., Spoelstra, T.A.T., and Blades, J.C. 1987, MNRAS, 228, 329

Somers, M.W. and Naylor, T. 1999, A&A, 352, 563

Szkody, P. and Howell, S.B. 1992, ApJS, 78, 537

Thorstensen, J.R. and Taylor, C.J. 2000, MNRAS, 312, 629

Tolbert, C.R., Pecker, J.C., and Pottasch, S.R. 1967, Bull. Astron. Inst. Netherlands, 19, 17

Tomaney, A.B. and Shafter, R.W. 1993, ApJ, 411, 640

Tylenda, R. 1977, Acta Astr., 27, 389

Vanlandingham, K.M, Starrfield, S., Wagner, R.M., Shore, S.N., and Sonneborn, G. 1996, MNRAS, 282, 563

Vanlandingham, K.M, Schwarz, G.J., Shore, S.N., and Starrfield, S. 2001, AJ, 121, 1126

Webster, B.L. 1969, MNRAS, 143, 79

Weiler, E.J. and Bahng, J.D.R. 1976, MNRAS, 174, 563

Whipple, F.H. and Payne-Gaposchkin, C. 1937, Harvard College Circ. 414

Whipple, F.H. and Payne-Gaposchkin, C. 1939, Harvard College Circ. 433

Whitney, B.A. and Clayton, G.C. 1989, AJ, 98, 297

Williams, R.E. 1982, ApJ, 261, 170

Williams, R.E. 1992, AJ, 104, 725

Williams, R.E. 1994, ApJ, 426, 279

Williams, R.E. 2000, private communication

Williams, R.E., Woolf, N.J., Hege, E.K., Moore, R.L., and Kopriva, D.A. 1978, ApJ, 224, 171

Williams, R.E., Phillips, M.M., and Hamuy, M. 1994, ApJS, 90, 297

Zhen-xi, Z. and Heng-rong, H. 2000 Chin. A&A, 24, 71

Zwitter, T. and Munari, U. 1995, A&AS, 114, 575

Zwitter, T. and Munari, U. 1996, A&AS, 117, 449

Table 1. Nova Characteristics

Object	t_2 days	t_3 days	Speed Class	Spectral Class	Peculiarity	Dist. pc	Ext. E_{B-V}	Dist. Ref.	Ext. Ref.	Flux data References
OS And	10	21	F			5100	0.25	(1)	(1)	(1,2)
DO Aql	430	900	S			6500	0.13	(3)	(3)	(4)
V603 Aql	4	9	VF	hy		330	0.07	(5)	(5)	(2,4,6,7)
V1229 Aql	20	38	MF	Fe		2100	0.50	(5)	(5)	(8)
V1370 Aql	9	13	F			5000	0.6	(90	(9)	(2,10)
V1419 Aql	19	32	F			2800	0.78	(3)	(11,12)	(13)
V1425 Aql	11	23	F	Fe		2700	0.76	(14)	(14)	(14)
T Aur	45	50	MF	Fe	dust	960	0.21	(5)	(5)	(3,6,15)
V365 Car	330	530	S			4700	0.85	(3)	(3)	(4)
V705 Cas	65	100	MF			3200	0.50	(16)	(16)	(13,17)
V723 Cas	19	180	S			3000	0.45	(18)	(18)	(19)
V812 Cen						10500	0.44	(20)	(20)	(4)
V842 Cen	35	48	MF	Fe	dust	1150	0.55	(5)	(5)	(4,21,22)
V868 Cen	55	?	MF	Fe		1900	1.75	(3)	(23)	(4,13)
V888 Cen	11	20	F			5000	0.84	(3)	(3)	(4,24)
IV Cep	16	36	F			5300	0.63	(20)	(20)	(6,25)
BY Cir	11	50	F			6000	0.73	(3)	(3)	(4)
CP Cru	4		VF			3200	0.63	(5)	(5)	(4)
Q Cyg	5	11	VF			1700	0.25	(20)	(20)	(6)
V450 Cyg	95/88?	108	MF	Fe		3500	0.41	(5)	(5)	(2)
V476 Cyg	6	15	VF	Fe		1620	0.26	(5)	(5)	(2,7,15,26)
V1500 Cyg	2	4	VF	hy		1500	0.50	(5)	(5)	(2,27,28)
V1819 Cyg	37	89	MF	Fe		7400	0.35	(5)	(5)	(4,29)
V1974 Cyg	17	37	F	Fe	ONeMg	1800	0.35	(5)	(5)	(4,30)
HR Del	172	230	VS	Fe		760	0.15	(5)	(5)	(2,3,4,6,31,32)
DN Gem	16	37	F			1600	0.10	(33)	(20)	(26)
DQ Her	39	86	MF	Fe	dust	480	0.1	(5)	(5)	(2,3,6,7,15,34,35,36)
V446 Her	7	12	F	He		1350	0.36	(5)	(5)	(6,17,37,38)
V533 Her	22	46	F	Fe		1250	0.0	(5)	(5)	(6,38)
V827 Her	25	60	MF			8500	0.16	(20)	(20)	(4)
V838 Her	2	5	VF	hy/He?	(neon)	3000	0.49	(39)	(39)	(13,39,40)
CP Lac	5	10	VF	hy		1350	0.20	(5)	(5)	(2,6,41)
DI Lac	20	43	MF			2600	0.16	(20)	(20)	(26)
DK Lac	11	24	F	Fe		3900	0.44	(5)	(5)	(2,6,42)
HY Lup		> 25	MF			1800	0.22	(5)	(5)	(4)
HR Lyr	45	74	S			4200	0.16	(20)	(20)	(15)
BT Mon	?	?	?			1800	0.15	(5)	(5)	(6,42)
GQ Mus	5	45	F-MF			4800	0.42	(43)	(43)	(4,23,43,44,45)
V841 Oph	50	145	MF			300	0.32	(20)	(20)	(6)
V972 Oph		176	S			2200	0.63	(20)	(20)	(2,4,46)
V2104 Oph						3300	0.06	(20)	(20)	(4)
V2214 Oph	56	92	MF	Fe	(neon)	1600	0.72	(47)	(23,47)	(4,13)
V2264 Oph	19	45	F	Fe	(neon)	6000	0.50	(47)	(23)	(13)
V2295 Oph	13	21	F			10000	0.40	(3)	(3)	(13)
GK Per	7	13	VF	He	neon!	455	0.3	(5)	(5)	(3,6,7,15)
V400 Per	20		F			13100	0.06	(20)	(20)	(48)

Table 1. Nova Characteristics (continued)

Object	t_2 days	t_3 days	Speed Class	Spectral Class	Peculiarity	Dist. pc	Ext. E_{B-V}	Dist. Ref.	Ext. Ref.	Flux data References
RR Pic	20	127	S	Fe		580	0.05	(5)	(5)	(4,15,49)
CP Pup	6	8	VF	He	neon?	1700	0.25	(5)	(5)	(4,15)
HS Pup		65	MF			5400	0.35	(20)	(20)	(50)
HZ Pup		70	MF			5800	0.25	(20)	(20)	(50)
V351 Pup	10	26	VF	Fe	ONeMg	2700	0.72	(5)	(5)	(4,13,51)
V630 Sgr	4	11	VF		neon!	600	0.51	(20)	(20)	(15)
V3888 Sgr	?	?	?			2500	1.02	(5)	(5)	(4)
V4157 Sgr	10	22	VF	Fe		7000	0.94	(3)	(23)	(13)
V4160 Sgr	6	14	VF	He	(neon)	5200	0.29	(20)	(20)	(13)
V4169 Sgr	22	43	F			6500	0.36	(52)	(52)	(13)
V4171 Sgr	17	31	F			4300	0.60	(3)	(23)	(13)
V4361 Sgr	> 30		MF/S			4500	1.38	(3)	(3)	(4)
V4444 Sgr	3.5		VF			4700	0.75	(53)	(53)	(4)
V4633 Sgr	16	35	F	Fe		7300	0.39	(3)	(3)	(4)
V4642 Sgr	?		MF?	Fe		7200	0.87	(3)	(3)	(4)
V960 Sco										(4)
V977 Sco	3	8	VF	Fe		10000	1.48	(3)	(3)	(13)
V992 Sco	?		MF			1600	0.72	(3)	(3)	(13)
V1141 Sco	3	7	VF			7200	1.26	(3)	(3)	(4)
V1142 Sco	8	12	VF			6000	0.74	(3)	(3)	(4)
FV Sct		?								(6)
V368 Sct	40	85	MF			3900	0.73	(20)	(20)	(54)
V373 Sct			MF			4600	0.32	(20)	(20)	(6)
V443 Sct	19	39	F	Fe		8000	0.27	(55)	(55)	(13,55)
V444 Sct	6	10	VF	Fe	neon?	8000	1.66	(3)	(3)	(13)
X Ser	370	555	VS			3000	0.25	(38)	(38)	(4,6,38)
CT Ser	?	?	F?			1400	0.01	(5)	(5)	(2,4,6,56)
FH Ser	42	59	MF	Fe	dust	920	0.64	(5)	(5)	(2,6,57)
LW Ser	40	50	MF			7900	0.32	(20)	(20)	(4)
XX Tau	24	42	F	Fe	dust	3500	0.40	(5)	(5)	
RW UMi	48	88	MF	Fe?		5000	0.09	(5)	(5)	(2,4)
LV Vul	21	43	F	Fe		920	0.56	(5)	(5)	(2)
NQ Vul	23	53	F	Fe		1160	0.67	(5)	(5)	(2,4,6)
PW Vul	82	126	S	Fe		1800	0.55	(5)	(5)	(2,4,58)
QU Vul	22	49	F	Fe	ONeMg	1750	0.60	(5)	(5)	(4,57,59,60)
QV Vul	50	53	MF	Fe		2700	0.40	(5)	(5)	(4,61,62)
recurrent novae										
V394 CrA	3.3	8	VF	He	recur	4200	1.10	(63)	(63)	(13)
RS Oph	4	14	VF		recur	570	0.73	(64)	(64)	(65,66)
T Pyx	62	88	MF		recur	4240	0.24	(67)	(67)	(4)
V3890 Sgr	9	18	VF	He	recur	3600	1.1	(68)	(68,69)	(13,69)
U Sco	2.0	4	VF		recur	7000	0.56	(70)	(70)	(71)
V745 Sco	6.6	10	VF	He	recur	8000	1.13	(72)	(23)	(13)

Table 1. Nova Characteristics (continued)

Object	t_2 days	t_3 days	Speed Class	Spectral Class	Peculiarity	Dist. pc	Ext. $E(B-V)$	Dist. Ref.	Ext. Ref.	Flux data References
extragalactic novae										
LMC 88-1	20	43	F	Fe		55 kpc	0.25		(23)	(13)
LMC 88-2	5		VF	Fe		55 kpc	0.25			(13)
LMC 90-1	8		VF	?	ONeMg	55 kpc	0.25			(13)
LMC 91	5	8	VF	Fe		55 kpc	0.25		(23)	(13)
LMC 92	9	14	VF			55 kpc	0.25		(23)	(13)
M31 C-31			S			770 kpc	0.11			(73,74,75)
M31 C-32	8	12	VF			770 kpc	0.11			(73,74)
extragalactic recurrent novae										
LMC 90-2	3	5	VF	He	recur	55 kpc	0.11		(76,77)	(13)

References to Table 1.

(1) Schwarz et al. (1997)
(2) Ringwald, Naylor & Mukai (1996)
(3) this work (new determination)
(4) this work (imaging)
(5) Downes & Duerbeck (2000)
(6) this work (spectroscopy)
(7) Payne-Gaposchkin & Gaposchkin (1942)
(8) Della Valle & Duerbeck (1993)
(9) Snijders et al. (1984)
(10) Snijders et al. (1987)
(11) Lynch et al. (1995)
(12) Munari et al. (1994)
(13) Williams (2000)
(14) Kamath et al. (1997)
(15) Payne-Gaposchkin (1957)
(16) Hauschild et al. (1994)
(17) Liu & Hu (2000)
(18) Munari et al. (1996)
(19) Hang, Zhu & Liu (1999)
(20) Shafter (1997)
(21) Andreä et al. (1994)
(22) de Freitas Pacheco et al. (1989)
(23) Williams (1994)
(24) Zhen-xi & Heng-rong (2000)
(25) Bahng (1972)
(26) McLaughlin (1953)
(27) Kałużny & Chlebowski (1988)
(28) Ferland et al. (1986)
(29) Whitney & Clayton (1989)
(30) Rafanelli et al. (1995)
(31) Tylenda (1977)
(32) Anderson & Gallagher (1977)
(33) Retter et al. (1999)
(34) Whipple & Payne-Gaposchkin (1937, 1939)
(35) Ferland et al. (1984)
(36) Mustel & Boyarchuk (1970)

References to Table 1 (continued)

(37) Honeycutt et al. (1995)
(38) Thorstensen & Taylor (2000)
(39) Vanlandingham et al. (1996)
(40) Matheson et al. (1993)
(41) Popper (1940)
(42) Larsson-Leander (1954)
(43) Diaz et al. (1995)
(44) Péquignot et al. (1993)
(45) Morisset & Péquignot (1995)
(46) Zwitter & Munari (1996)
(47) Lynch et al. (1989)
(48) Weiler & Bahng (1976)
(49) Payne-Gaposchkin & Menzel (1938)
(50) Zwitter & Munari (1995)
(51) Saizar et al. (1996)
(52) Scott et al. (1995)
(53) Kawabata et al. (2000)
(54) Ciatti & Rosino (1974)
(55) Anupama et al. (1992)
(56) Szkody & Howell (1992)
(57) Della Valle et al. (1997)
(58) Saizar et al. (1991)
(59) Rosino et al. (1992)
(60) Saizar et al. (1992)
(61) Scott et al. (1994)
(62) Gehrz et al. (1992)
(63) Hachisu & Kato (2000a)
(64) Hachisu & Kato (2000b)
(65) Tolbert et al. (1967)
(66) Bohigas et al. (1989)
(67) Gilmozzi et al. (1998)
(68) González-Riestra (1992)
(69) Anupama & Sethi (1994)
(70) Hachisu et al. (2000)
(71) Anupama & Dewangan (2000)
(72) Sekiguchi et al. (1990a)
(73) Ciardullo et al. (1987)
(74) Ciardullo et al. (1990)
(75) Tomaney & Shafter (1993)
(76) Shore et al. (1991)
(77) Sekiguchi et al. (1990b)

Table 2. [O III] λ5007 Flux and Luminosity

Object	Age (years)	Flux (erg cm^{-2} s^{-1})	Ref.	Luminosity (erg s^{-1})
OS And	4.6	3.4×10^{-14}	(2)	2.5×10^{32}
DO Aql	74.9	9.3×10^{-15}	(4)	7.3×10^{31}
V603 Aql	59.8[a]	2.1×10^{-14}	(6)	3.5×10^{29}
	0.89	4.9×10^{-7}	(7)	8.2×10^{36}
	0.46	4.7×10^{-7}	(7)	7.9×10^{36}
	0.33	3.5×10^{-7}	(7)	5.9×10^{36}
	0.31	4.6×10^{-7}	(7)	7.7×10^{36}
	0.29	4.2×10^{-7}	(7)	7.0×10^{36}
	0.27	3.7×10^{-7}	(7)	6.2×10^{36}
	0.25	4.2×10^{-7}	(7)	7.0×10^{36}
	0.23	4.8×10^{-7}	(7)	8.0×10^{36}
	0.21	3.9×10^{-7}	(7)	6.5×10^{36}
	0.19	3.0×10^{-7}	(7)	5.0×10^{36}
	0.18	3.7×10^{-7}	(7)	6.2×10^{36}
	0.17	4.4×10^{-7}	(7)	7.4×10^{36}
	0.16	3.8×10^{-7}	(7)	6.4×10^{36}
	0.15	3.6×10^{-7}	(7)	6.0×10^{36}
	0.14	5.3×10^{-7}	(7)	8.9×10^{36}
	0.13	3.8×10^{-7}	(7)	6.4×10^{36}
	0.12	2.9×10^{-7}	(7)	4.9×10^{36}
	0.09	2.9×10^{-7}	(7)	4.9×10^{36}
	0.07	2.3×10^{-7}	(7)	3.9×10^{36}
V1229 Aql	22.2	absent	(8)	
V1370 Aql	9.5	absent	(2)	
	0.43	2.9×10^{-13}	(10)	6.1×10^{33}
V1419 Aql	0.118	absent	(13)	
V1425 Aql	2.31	3.2×10^{-13}	(14)	3.5×10^{33}
	0.31	4.0×10^{-11}	(14)	4.3×10^{35}
	0.20	6.8×10^{-11}	(14)	7.4×10^{35}
	0.14	3.9×10^{-11}	(14)	4.2×10^{35}
	0.14	3.1×10^{-11}	(14)	3.4×10^{35}
T Aur	94.0	absent	(4)	
	87.2[a]	1.9×10^{-15}	(6)	4.2×10^{29}
	11.7	absent	(15)	
	9.8	present	(15)	
V705 Cas	5.0	1.6×10^{-12}	(17)	1.0×10^{34}
V705 Cas	0.186	absent	(13)	
V723 Cas	2.3	2.6×10^{-12}	(19)	1.2×10^{34}
V812 Cen	25.0	absent	(4)	
V842 Cen	13.7	4.1×10^{-14}	(4)	4.0×10^{31}
	11.3	1.5×10^{-13}	(4)	1.5×10^{32}
	4.6	present	(21)	
	1.3	2.4×10^{-9}	(22)	2.3×10^{36}
	0.7	4.0×10^{-9}	(22)	3.9×10^{36}
	0.6	3.9×10^{-9}	(22)	3.8×10^{36}
V868 Cen	7.0	2.0×10^{-14}	(4)	2.7×10^{33}
	2.060	3.9×10^{-12}	(13)	5.3×10^{35}
	1.975	3.3×10^{-12}	(13)	4.5×10^{35}
	1.830	2.2×10^{-12}	(13)	3.0×10^{35}
	1.328	8.6×10^{-13}	(13)	1.2×10^{35}
	0.925	6.7×10^{-13}	(13)	9.2×10^{34}
	0.767	4.9×10^{-13}	(13)	6.7×10^{34}
	0.263	absent	(13)	
	0.194	absent	(13)	
	0.112	absent	(13)	
	0.099	absent	(13)	
	0.082	absent	(13)	
	0.063	absent	(13)	
	0.043	absent	(13)	
	0.003	absent	(13)	

Table 2. [O III] λ5007 Flux and Luminosity (continued)

Object	Age (years)	Flux (erg cm^{-2} s^{-1})	Ref.	Luminosity (erg s^{-1})
V888 Cen	3.1	2.1×10^{-13}	(4)	1.0×10^{34}
	2.8	2.6×10^{-12}	(24)	1.3×10^{34}
IV Cep	13.1	absent	(4)	
	8.3[a]	3.9×10^{-16}	(6)	1.1×10^{31}
	0.31	1.6×10^{-11}	(25)	4.4×10^{35}
	0.21	1.6×10^{-11}	(25)	4.4×10^{35}
BY Cir	3.2	1.6×10^{-12}	(4)	7.7×10^{34}
CP Cru	1.6	2.7×10^{-14}	(4)	2.7×10^{32}
Q Cyg	103.[a]	1.9×10^{-15}	(6)	1.5×10^{30}
V476 Cyg	64.0	absent	(4)	
	17.8	absent	(15)	
	15.8	present	(26)	
	2.7	present	(26)	
	0.15	8.1×10^{-9}	(7)	6.1×10^{36}
	0.13	9.6×10^{-9}	(7)	7.3×10^{36}
	0.12	7.8×10^{-9}	(7)	5.9×10^{36}
	0.11	9.9×10^{-9}	(7)	7.5×10^{36}
	0.09	1.7×10^{-8}	(7)	1.3×10^{37}
	0.08	1.9×10^{-8}	(7)	1.4×10^{37}
V1500 Cyg	11.8	absent	(27)	
	9.0	1.5×10^{-15}	(4)	2.2×10^{30}
	0.98	7.8×10^{-11}	(28)	1.1×10^{35}
	0.81	7.7×10^{-11}	(28)	1.1×10^{35}
	0.73	1.5×10^{-10}	(28)	2.2×10^{35}
	0.38	1.8×10^{-10}	(28)	2.6×10^{35}
	0.33	2.4×10^{-10}	(28)	3.5×10^{35}
	0.28	3.1×10^{-10}	(28)	4.5×10^{35}
	0.24	3.6×10^{-10}	(28)	5.2×10^{35}
	0.21	4.2×10^{-10}	(28)	6.1×10^{35}
	0.19	4.6×10^{-10}	(28)	6.6×10^{35}
	0.16	5.0×10^{-10}	(28)	7.2×10^{35}
	0.13	6.1×10^{-10}	(28)	8.8×10^{35}
	0.10	6.6×10^{-10}	(28)	9.5×10^{35}
V1819 Cyg	11.8	2.2×10^{-15}	(4)	4.6×10^{31}
	1.8	3.0×10^{-12}	(29)	6.3×10^{34}
	0.9	5.2×10^{-11}	(29)	1.1×10^{36}
	0.3	absent	(29)	
V1974 Cyg	6.3	2.4×10^{-14}	(4)	3.0×10^{31}
	1.8	9.7×10^{-12}	(30)	1.2×10^{34}
	1.7	1.5×10^{-12}	(30)	1.9×10^{33}
	1.4	1.5×10^{-11}	(30)	1.9×10^{34}
	1.1	6.0×10^{-11}	(30)	7.4×10^{34}
	0.7	2.5×10^{-10}	(30)	3.1×10^{35}
HR Del	33.0	1.7×10^{-13}	(4)	2.0×10^{31}
	29.9	3.9×10^{-13}	(4)	4.5×10^{31}
	23.1	8.7×10^{-13}	(2)	1.0×10^{32}
	17.1	1.8×10^{-12}	(4)	2.0×10^{32}
	10.8	4.6×10^{-12}	(6)	5.3×10^{32}
	8.1	4.7×10^{-11}	(32)	5.4×10^{33}
	6.683	2.7×10^{-11}	(3)	3.1×10^{33}
	6.426	3.1×10^{-11}	(3)	3.6×10^{33}
	4.9	5.3×10^{-10}	(31)	6.1×10^{34}
	4.684	1.3×10^{-10}	(3)	1.5×10^{34}
	2.0	3.4×10^{-9}	(31)	3.9×10^{35}
	1.741	6.4×10^{-10}	(3)	7.3×10^{34}
	1.667	1.5×10^{-9}	(3)	1.7×10^{35}
HR Del	0.964	4.3×10^{-9}	(3)	4.9×10^{35}
	0.693	5.4×10^{-9}	(3)	6.1×10^{35}
	0.222	9.3×10^{-10}	(3)	1.1×10^{36}

Table 2. [O III] λ5007 Flux and Luminosity (continued)

Object	Age (years)	Flux (erg cm^{-2} s^{-1})	Ref.	Luminosity (erg s^{-1})
DN Gem	2.9	absent	(26)	
	1.9	present	(26)	
DQ Her	60.4[a]	5.5×10^{-15}	(6)	2.2×10^{29}
	49.8	1.2×10^{-13}	(3)	4.6×10^{30}
	49.7	7.6×10^{-14}	(4)	4.0×10^{30}
	43.4[a]	4.3×10^{-15}	(6)	1.7×10^{29}
	15.0	present	(15)	
	5.0	present	(15)	
	1.69	7.1×10^{-9}	(34)	2.8×10^{35}
	0.84	7.8×10^{-9}	(34)	3.1×10^{35}
	0.60	4.5×10^{-9}	(34)	1.8×10^{35}
	0.54	3.3×10^{-9}	(34)	1.3×10^{35}
	0.44	9.5×10^{-10}	(34)	3.7×10^{34}
V446 Her	33.4	absent	(37)	
V533 Her	15.2[a]	1.6×10^{-15}	(6)	3.1×10^{29}
V827 Her	12.4	5.7×10^{-16}	(4)	8.5×10^{30}
V838 Her	7.2	absent	(4)	
	1.5	absent	(40)	
	0.61	2.0×10^{-14}	(40)	1.1×10^{32}
	0.53	3.2×10^{-14}	(40)	1.8×10^{32}
	0.44	3.4×10^{-14}	(13)	1.9×10^{32}
	0.42	6.3×10^{-14}	(40)	3.5×10^{32}
	0.37	1.3×10^{-14}	(40)	7.2×10^{31}
	0.28	1.6×10^{-13}	(13)	8.8×10^{32}
	0.22	1.6×10^{-13}	(13)	8.8×10^{32}
	0.12	4.1×10^{-13}	(13)	2.3×10^{33}
	0.11	6.8×10^{-13}	(40)	3.8×10^{33}
	0.09	absent	(13)	
	0.05	4.9×10^{-12}	(40)	2.7×10^{34}
	0.027	absent	(13)	
CP Lac	49.0	absent	(4)	
	43.3[a]	9.0×10^{-16}	(6)	3.9×10^{29}
	0.42	8.8×10^{-10}	(41)	3.8×10^{35}
	0.32	1.3×10^{-9}	(41)	5.7×10^{35}
	0.26	1.4×10^{-9}	(41)	6.1×10^{35}
	0.18	1.6×10^{-9}	(41)	7.0×10^{35}
	0.13	1.9×10^{-9}	(41)	8.3×10^{35}
	0.10	2.3×10^{-9}	(41)	1.0×10^{36}
	0.07	1.4×10^{-9}	(41)	6.1×10^{35}
DI Lac	25.7	absent	(26)	
	2.9	present	(26)	
DK Lac	29.8[a]	4.2×10^{-16}	(6)	3.4×10^{30}
	0.30		(42)	5.3×10^{34}
	0.24		(42)	7.7×10^{34}
	0.21		(42)	6.6×10^{34}
	0.16		(42)	1.8×10^{35}
HY Lup	4.5	7.7×10^{-14}	(4)	6.3×10^{31}
HR Lyr	16.5	absent	(15)	
BT Mon	42.2	absent	(31)	
	40.1[a]	1.6×10^{-15}	(6)	1.0×10^{30}
GQ Mus	15.2	absent	(4)	
	11.1	9.2×10^{-16}	(43)	1.0×10^{31}
	9.01	absent	(13,43)	
	8.84	absent	(13)	
	7.51	absent	(13,43)	
	7.36	absent	(13)	
GQ Mus	5.39	absent	(13)	
	4.0	absent	(44)	
	3.4	4.6×10^{-14}	(45)	5.2×10^{32}
	3.1	2.1×10^{-13}	(45)	2.4×10^{33}

Table 2. [O III] λ5007 Flux and Luminosity (continued)

Object	Age (years)	Flux (erg cm^{-2} s^{-1})	Ref.	Luminosity (erg s^{-1})
GQ Mus	2.3	1.6×10^{-11}	(45)	1.8×10^{35}
	1.4	1.3×10^{-10}	(45)	1.5×10^{36}
	1.2	1.5×10^{-10}	(45)	1.7×10^{36}
V841 Oph	130.[a]	9.7×10^{-15}	(6)	
V972 Oph	42.8	absent	(4)	
	37.6	absent	(46)	
V2014 Oph	21.7	absent	(4)	
V2214 Oph	13.3	3.9×10^{-15}	(4)	1.3×10^{31}
	2.984	absent	(13)	
	2.080	absent	(13)	
	1.918	absent	(13)	
	1.455	absent	(13)	
	1.104	absent	(13)	
	0.485	absent	(13)	
	0.455	absent	(13)	
	0.364	absent	(13)	
	0.274	absent	(13)	
	0.238	absent	(13)	
	0.206	absent	(13)	
	0.200	absent	(13)	
	0.164	absent	(13)	
	0.162	absent	(13)	
	0.107	absent	(13)	
	0.104	absent	(13)	
	0.101	absent	(13)	
	0.071	absent	(13)	
V2264 Oph	1.301	7.4×10^{-13}	(13)	4.2×10^{34}
	1.088	5.3×10^{-13}	(13)	3.0×10^{34}
	0.904	1.1×10^{-12}	(13)	6.2×10^{34}
	0.397	1.5×10^{-12}	(13)	8.5×10^{34}
	0.232	1.3×10^{-12}	(13)	7.3×10^{34}
	0.173	absent	(13)	
	0.118	absent	(13)	
	0.077	absent	(13)	
	0.041	absent	(13)	
	0.027	absent	(13)	
V2295 Oph	0.038	absent	(13)	
GK Per	84.0	8.3×10^{-13}	(4)	5.7×10^{31}
	83.6	8.2×10^{-13}	(3)	5.6×10^{31}
	78.7[a]	8.7×10^{-15}	(6)	5.9×10^{29}
	3.9	absent	(15)	
	1.44	2.4×10^{-9}	(7)	1.6×10^{35}
	0.74	5.5×10^{-9}	(7)	3.7×10^{35}
	0.57	1.6×10^{-8}	(7)	1.1×10^{36}
	0.48	3.1×10^{-8}	(7)	2.1×10^{36}
	0.39	2.5×10^{-8}	(7)	1.7×10^{36}
	0.34	3.5×10^{-8}	(7)	2.4×10^{36}
	0.29	4.5×10^{-8}	(7)	3.1×10^{36}
	0.17	1.9×10^{-8}	(7)	1.3×10^{36}
V400 Per	0.46	1.1×10^{-11}	(48)	2.9×10^{35}
	0.44	1.1×10^{-11}	(48)	2.9×10^{35}
	0.35	1.9×10^{-11}	(48)	4.9×10^{35}
RR Pic	72.8	7.4×10^{-14}	(4)	3.6×10^{30}
	6.0	absent	(15)	
	3.66	3.0×10^{-9}	(49)	1.5×10^{35}
	2.86	4.3×10^{-9}	(49)	2.1×10^{35}
	2.56	5.2×10^{-9}	(49)	2.5×10^{35}
	1.87	7.7×10^{-9}	(49)	3.7×10^{35}
	1.79	7.2×10^{-9}	(49)	3.5×10^{35}
	1.75	8.0×10^{-9}	(49)	3.9×10^{35}

Table 2. [O III] λ5007 Flux and Luminosity (continued)

Object	Age (years)	Flux (erg cm^{-2} s^{-1})	Ref.	Luminosity (erg s^{-1})
RR Pic	1.49	5.6×10^{-9}	(49)	2.7×10^{35}
	1.38	4.2×10^{-9}	(49)	2.0×10^{35}
	1.32	5.9×10^{-9}	(49)	2.9×10^{35}
	1.25	4.3×10^{-9}	(49)	2.1×10^{35}
	1.15	3.1×10^{-9}	(49)	1.5×10^{35}
	0.99	4.9×10^{-9}	(49)	2.4×10^{35}
	0.95	4.4×10^{-9}	(49)	2.1×10^{35}
	0.91	3.4×10^{-9}	(49)	1.7×10^{35}
	0.88	3.6×10^{-9}	(49)	1.8×10^{35}
	0.85	5.2×10^{-9}	(49)	2.5×10^{35}
	0.74	3.2×10^{-9}	(49)	1.6×10^{35}
	0.66	4.4×10^{-9}	(49)	2.1×10^{35}
CP Pup	52.9	9.3×10^{-14}	(4)	7.5×10^{31}
	3.4	present	(15)	
HS Pup	30.8	absent	(50)	
HZ Pup	31.7	absent	(50)	
V351 Pup	6.1	5.9×10^{-15}	(4)	5.7×10^{31}
	1.325	9.5×10^{-12}	(13)	9.2×10^{34}
	1.3	9.5×10^{-12}	(51)	9.2×10^{34}
	1.237	1.3×10^{-11}	(13)	1.3×10^{35}
	1.2	1.3×10^{-11}	(51)	1.3×10^{35}
	1.011	2.4×10^{-11}	(13)	2.3×10^{35}
	1.0	2.5×10^{-11}	(51)	2.4×10^{35}
	0.4	5.2×10^{-11}	(51)	5.0×10^{35}
	0.375	4.7×10^{-11}	(13)	4.6×10^{35}
	0.189	absent	(13)	
	0.112	absent	(13)	
	0.088	absent	(13)	
	0.030	absent	(13)	
V630 Sgr	0.8	present	(15)	
V4157 Sgr	1.367	7.7×10^{-13}	(13)	9.5×10^{34}
	1.186	9.9×10^{-13}	(13)	1.2×10^{35}
	1.107	1.4×10^{-12}	(13)	1.7×10^{35}
	0.778	1.9×10^{-12}	(13)	2.4×10^{35}
	0.463	3.6×10^{-12}	(13)	4.5×10^{35}
	0.386	1.2×10^{-12}	(13)	1.5×10^{35}
	0.244	2.7×10^{-11}	(13)	3.4×10^{36}
	0.104	absent	(13)	
	0.060	absent	(13)	
	0.016	absent	(13)	
V4160 Sgr	0.197	3.6×10^{-13}	(13)	3.1×10^{33}
	0.096	absent	(13)	
	0.008	absent	(13)	
V4169 Sgr	0.956	2.5×10^{-12}	(13)	4.2×10^{34}
	0.786	4.3×10^{-12}	(13)	7.2×10^{34}
	0.700	6.0×10^{-12}	(13)	1.0×10^{35}
	0.295	1.6×10^{-11}	(13)	2.7×10^{35}
	0.053	absent	(13)	
V4171 Sgr	0.701	2.8×10^{-12}	(13)	4.5×10^{34}
	0.529	6.1×10^{-12}	(13)	9.8×10^{34}
	0.441	1.4×10^{-11}	(13)	2.3×10^{35}
	0.189	absent	(13)	
	0.110	absent	(13)	
	0.038	absent	(13)	
V4361 Sgr	1.7	7.7×10^{-13}	(4)	1.8×10^{35}
V4444 Sgr	1.2	5.5×10^{-13}	(4)	1.7×10^{34}
V4633 Sgr	2.3	6.4×10^{-13}	(4)	1.5×10^{34}
V4642 Sgr	0.5	6.2×10^{-13}	(4)	6.8×10^{34}
V960 Sco	14.8	1×10^{-16}:	(4)	
V977 Sco	2.630	1.6×10^{-14}	(13)	2.5×10^{34}

Table 2. [O III] λ5007 Flux and Luminosity (continued)

Object	Age (years)	Flux (erg cm^{-2} s^{-1})	Ref.	Luminosity (erg s^{-1})
V977 Sco	1.819	5.0×10^{-14}	(13)	7.7×10^{34}
	1.000	1.4×10^{-12}	(13)	2.2×10^{36}
	0.805	7.8×10^{-13}	(13)	1.2×10^{36}
	0.750	7.4×10^{-13}	(13)	1.1×10^{36}
	0.666	9.0×10^{-13}	(13)	1.4×10^{36}
	0.630	8.0×10^{-13}	(13)	1.2×10^{36}
	0.520	7.3×10^{-13}	(13)	1.1×10^{36}
	0.129	absent	(13)	
	0.079	absent	(13)	
	0.014	absent	(13)	
V992 Sco	1.090	1.8×10^{-11}	(13)	6.0×10^{34}
	0.923	1.9×10^{-11}	(13)	6.3×10^{34}
	0.189	absent	(13)	
	0.830	1.9×10^{-11}	(13)	6.3×10^{34}
	0.427	absent	(13)	
	0.205	absent	(13)	
	0.186	absent	(13)	
	0.181	absent	(13)	
	0.175	absent	(13)	
	0.164	absent	(13)	
	0.159	absent	(13)	
	0.153	absent	(13)	
	0.137	absent	(13)	
	0.131	absent	(13)	
	0.126	absent	(13)	
	0.121	absent	(13)	
	0.115	absent	(13)	
	0.110	absent	(13)	
	0.104	absent	(13)	
	0.099	absent	(13)	
	0.077	absent	(13)	
	0.046	absent	(13)	
	0.033	absent	(13)	
	0.022	absent	(13)	
V1141 Sco	3.1	absent	(4)	
	0.8	3.5×10^{-14}	(4)	1.3×10^{34}
V1142 Sco	1.7	3.2×10^{-14}	(4)	1.6×10^{33}
FV Sct	31.1	absent	(2)	
V368 Sct	3.2	present	(53)	
V373 Sct	16.1	absent	(2)	
V443 Sct	3.060	1.8×10^{-13}	(13)	5.2×10^{33}
	1.767	7.4×10^{-13}	(13)	2.1×10^{34}
	1.038	4.0×10^{-12}	(13)	1.2×10^{35}
	0.742	7.1×10^{-12}	(13)	2.1×10^{35}
	0.687	5.1×10^{-12}	(13)	1.5×10^{35}
	0.602	8.3×10^{-12}	(13)	2.4×10^{35}
	0.192	absent	(13)	
	0.066	absent	(13)	
V444 Sct	0.591	4.8×10^{-15}	(13)	8.5×10^{33}
	0.186	absent	(13)	
	0.110	absent	(13)	
	0.006	absent	(13)	
X Ser	97.2	2.4×10^{-15}:	(4)	6.1×10^{30}
	74.9[a]	6.7×10^{-16}	(1)	1.7×10^{30}
CT Ser	52.5	absent	0	
	47.0[a]	5.8×10^{-16}	(6)	1.4×10^{29}
FH Ser	24.1	present	(57)	
	20.5	4.0×10^{-15}	(2)	3.6×10^{30}
	14.5	2.8×10^{-15}	(4)	2.4×10^{30}
	9.7	5.1×10^{-14}	(6)	4.6×10^{31}

Table 2. [O III] λ5007 Flux and Luminosity (continued)

Object	Age (years)	Flux (erg cm^{-2} s^{-1})	Ref.	Luminosity (erg s^{-1})
LW Ser	22.4	2.3×10^{-15}	(4)	
XX Tau	56.9	absent	(4)	
RW UMi	41.7	absent	(4)	
	27.9	absent	(4)	
LV Vul	23.3	absent	(2)	
NQ Vul	21.6[a]	9.4×10^{-16}	(6)	1.4×10^{30}
	14.7	2.0×10^{-15}	(2)	2.9×10^{30}
	0.186	absent	(13)	
PW Vul	13.8	1.7×10^{-15}	(4)	4.1×10^{30}
	7.0	8.3×10^{-14}	(2)	2.0×10^{32}
	2.8	3.9×10^{-12}	(58)	9.3×10^{33}
	1.9	1.2×10^{-11}	(58)	2.9×10^{34}
	1.7	1.2×10^{-11}	(58)	2.9×10^{34}
	1.1	6.0×10^{-11}	(58)	1.4×10^{35}
	0.8	5.7×10^{-11}	(58)	1.4×10^{35}
	0.6	6.4×10^{-11}	(58)	1.5×10^{35}
QU Vul	13.5	3.6×10^{-14}	(4)	9.7×10^{31}
	9.5	9.4×10^{-14}	(57)	2.5×10^{32}
	5.7	5.9×10^{-13}	(59)	1.6×10^{33}
	3.7	5.0×10^{-12}	(59)	1.3×10^{34}
	2.92	1.8×10^{-12}	(60)	4.8×10^{33}
	2.83	3.2×10^{-12}	(60)	8.5×10^{33}
	2.70	4.6×10^{-12}	(60)	1.2×10^{34}
	2.6	1.7×10^{-11}	(59)	4.6×10^{34}
	2.51	5.3×10^{-12}	(60)	1.4×10^{34}
	2.41	5.8×10^{-12}	(60)	1.6×10^{34}
	2.36	6.3×10^{-12}	(60)	1.7×10^{34}
	2.25	9.1×10^{-12}	(60)	2.4×10^{34}
	1.79	1.3×10^{-11}	(60)	3.5×10^{34}
	1.78	1.1×10^{-11}	(60)	3.0×10^{34}
	1.75	1.1×10^{-11}	(60)	3.0×10^{34}
	1.68	1.6×10^{-11}	(60)	4.2×10^{34}
	1.59	1.6×10^{-11}	(60)	4.2×10^{34}
	1.54	1.5×10^{-11}	(60)	4.1×10^{34}
	1.45	1.7×10^{-11}	(60)	4.6×10^{34}
	1.32	1.4×10^{-11}	(60)	3.8×10^{34}
	0.85	1.8×10^{-11}	(60)	4.9×10^{34}
	0.71	1.9×10^{-11}	(60)	5.0×10^{34}
	0.39	1.5×10^{-11}	(60)	3.9×10^{34}
QV Vul	10.5	1.7×10^{-14}	(4)	5.6×10^{31}
	5.71	5.6×10^{-13}	(61)	1.9×10^{33}
	2.79	2.7×10^{-11}	(62)	8.8×10^{34}
recurrent	novae			
V394 CrA	0.077	absent	(13)	
	0.058	absent	(13)	
V394 CrA	0.021	absent	(13)	
	0.015	absent	(13)	
RS Oph	0.551	4.1×10^{-12}	(66)	1.8×10^{33}
	0.118	6.4×10^{-12}	(67)	2.8×10^{33}
	0.107	1.1×10^{-11}	(67)	4.8×10^{33}
	0.091	9.0×10^{-12}	(67)	3.9×10^{33}
	0.069	6.4×10^{-12}	(67)	2.8×10^{33}
T Pyx	31.3	1.8×10^{-14}	(4)	8.6×10^{31}
V3890 Sgr	1.044	absent	(13)	
	0.501	1.5×10^{-13}	(13)	9.3×10^{33}
	0.411	1.9×10^{-13}	(13)	1.2×10^{34}
	0.241	2.5×10^{-13}	(13)	1.6×10^{34}
	0.183	2.5×10^{-13}	(13)	1.6×10^{34}
	0.112	absent	(13)	

Table 2. [O III] λ5007 Flux and Luminosity (continued)

Object	Age (years)	Flux (erg cm^{-2} s^{-1})	Ref.	Luminosity (erg s^{-1})
V3890 Sgr	0.093	absent	(13)	
	0.077	absent	(13)	
	0.049	absent	(69)	
	0.024	absent	(13)	
U Sco	0.032	absent	(71)	
V745 Sco	2.679	absent	(13)	
	1.868	3.4×10^{-15}	(13)	7.5×10^{32}
	0.868	3.1×10^{-14}	(13)	6.8×10^{33}
	0.835	1.9×10^{-14}	(13)	4.2×10^{33}
	0.819	8.9×10^{-14}	(13)	2.0×10^{34}
	0.126	absent	(13)	
	0.060	absent	(13)	
	0.027	absent	(13)	
	0.016	absent	(13)	
	0.006	absent	(13)	
LMC novae				
1988-1	0.088	absent	(13)	
	0.047	absent	(13)	
	0.022	absent	(13)	
1988-2	0.099	absent	(13)	
	0.038	absent	(13)	
	0.014	absent	(13)	
	0.008	absent	(13)	
1990-1	0.058	absent	(13)	
	0.027	absent	(13)	
	0.011	absent	(13)	
1991	0.786	1.0×10^{-13}	(13)	8.5×10^{34}
	0.706	1.4×10^{-13}	(13)	1.2×10^{35}
	0.539	1.3×10^{-13}	(13)	1.1×10^{35}
	0.359	9.8×10^{-14}	(13)	8.3×10^{34}
	0.038	absent	(13)	
	0.003	absent	(13)	
1992	0.356	3.9×10^{-13}	(13)	3.3×10^{35}
	0.214	7.7×10^{-13}	(13)	6.5×10^{35}
	0.131	6.5×10^{-13}	(13)	5.5×10^{35}
	0.096	absent	(13)	
	0.052	absent	(13)	
	0.038	absent	(13)	
M31 novae				
C-32	4.7	1.99×10^{-15}	(75)	5.0×10^{34}
	3.6	1.39×10^{-15}	(75)	3.5×10^{34}
	2.7	1.71×10^{-15}	(75)	4.4×10^{34}
	1.7	1.23×10^{-15}	(75)	3.1×10^{34}

[a]spectrum with no emission present

Table 3. Hα Flux and Luminosity

Object	Age (years)	Flux (erg cm^{-2} s^{-1})	Ref.	Luminosity (erg s^{-1})
OS And	4.6	8.4×10^{-14}	(2)	4.7×10^{32}
DO Aql	74.9	1.5×10^{-14}	(4)	1.0×10^{32}
V603 Aql	78.0	5.7×10^{-13}	(6)??	8.9×10^{30}
	76.9	5.5×10^{-13}	(6)??	8.6×10^{30}
	72.2	7.0×10^{-13}	(2)	1.1×10^{31}
V1370 Aql	9.5	6.7×10^{-15}	(2)	8.1×10^{31}
	0.43	2.0×10^{-12}	(10)	2.4×10^{34}
V1419 Aql	0.118	6.4×10^{-11}	(13)	3.6×10^{35}
V1425 Aql	2.31[a]	1.8×10^{-13}	(14)	9.2×10^{32}
	0.31	7.7×10^{-11}	(14)	4.0×10^{35}
	0.20	4.3×10^{-10}	(14)	2.2×10^{36}
	0.14	5.6×10^{-10}	(14)	2.9×10^{36}
T Aur	94.0	2.9×10^{-14}	(4)	5.3×10^{30}
V365 Car	49.5	3.5×10^{-15}	(4)	6.7×10^{31}
V705 Cas	0.186	1.3×10^{-11}	(13)	5.2×10^{34}
V723 Cas	2.3	5.4×10^{-11}	(19)	1.7×10^{35}
	1.2	3.3×10^{-10}	(19)	1.1×10^{36}
	0.1	3.2×10^{-11}	(19)	9.8×10^{34}
V812 Cen	25.0	2.7×10^{-15}	(4)	9.9×10^{31}
V842 Cen	13.7	3.2×10^{-13}	(4)	1.8×10^{32}
	11.3	1.3×10^{-12}	(4)	7.4×10^{32}
	1.3	3.9×10^{-12}	(22)	2.2×10^{33}
	0.7	1.4×10^{-11}	(22)	7.0×10^{33}
	0.6	2.4×10^{-11}	(22)	1.4×10^{34}
V868 Cen	2.060	5.1×10^{-13}	(13)	1.4×10^{34}
	1.975	6.0×10^{-13}	(13)	1.6×10^{34}
	1.830	7.6×10^{-13}	(13)	2.1×10^{34}
	1.328	2.0×10^{-12}	(13)	5.4×10^{34}
	0.925	5.5×10^{-12}	(13)	1.5×10^{35}
	0.767	1.3×10^{-11}	(13)	8.4×10^{35}
	0.263	2.8×10^{-11}	(13)	7.6×10^{35}
	0.194	8.2×10^{-12}	(13)	2.2×10^{35}
	0.112	1.2×10^{-10}	(13)	3.3×10^{36}
	0.099	1.6×10^{-10}	(13)	4.3×10^{36}
	0.082	3.9×10^{-11}	(13)	1.1×10^{36}
	0.063	6.5×10^{-11}	(13)	1.8×10^{36}
	0.049	6.8×10^{-11}	(13)	1.8×10^{36}
	0.003	1.3×10^{-11}	(13)	3.5×10^{35}
V888 Cen	3.1	9.1×10^{-14}	(4)	1.9×10^{33}
IV Cep	13.1	1.4×10^{-15}	(4)	2.0×10^{31}
BY Cir	3.2	1.8×10^{-12}	(4)	4.2×10^{34}
CP Cru	1.6	3.1×10^{-14}	(4)	1.7×10^{32}
V450 Cyg	48.8	6.0×10^{-16}	(2)	2.3×10^{30}
V476 Cyg	64.0	6.0×10^{-15}	(4)	3.5×10^{30}
	42.2	7.3×10^{-15}	(2)	4.3×10^{30}
V1500 Cyg	14.9	1.6×10^{-14}	(2)	1.4×10^{31}
	8.95	9.7×10^{-15}	(4)	8.5×10^{30}
	0.98	2.0×10^{-11}	(28)	1.8×10^{34}
	0.81	2.1×10^{-11}	(28)	1.8×10^{34}
	0.73	4.2×10^{-11}	(28)	3.7×10^{34}
	0.38	8.3×10^{-11}	(28)	7.3×10^{34}
	0.33	1.2×10^{-10}	(28)	1.1×10^{35}
	0.28	2.1×10^{-10}	(28)	1.8×10^{35}
	0.24	3.4×10^{-10}	(28)	3.0×10^{35}
	0.22	5.3×10^{-10}	(28)	4.7×10^{35}
	0.19	6.7×10^{-10}	(28)	5.9×10^{35}
	0.16	1.1×10^{-09}	(28)	9.7×10^{35}
	0.13	2.1×10^{-09}	(28)	1.8×10^{36}
	0.10	3.4×10^{-09}	(28)	3.0×10^{36}
	0.08	6.1×10^{-09}	(28)	5.4×10^{36}

Table 3. Hα Flux and Luminosity (continued)

Object	Age (years)	Flux (erg cm^{-2} s^{-1})	Ref.	Luminosity (erg s^{-1})
V1500 Cyg	0.05	1.4×10^{-08}	(28)	1.2×10^{37}
	0.01	5.9×10^{-08}	(28)	5.2×10^{37}
V1819 Cyg	11.8	8.8×10^{-15}	(4)	1.3×10^{32}
	1.8	8.9×10^{-13}	(29)	1.3×10^{34}
	0.9	8.2×10^{-11}	(29)	2.2×10^{36}
	0.3	6.6×10^{-11}	(29)	9.8×10^{35}
	0.3	1.5×10^{-10}	(29)	2.2×10^{36}
	0.2	7.7×10^{-11}	(29)	1.2×10^{36}
	0.2	1.1×10^{-10}	(29)	1.6×10^{36}
	0.1	1.1×10^{-10}	(29)	1.6×10^{36}
	0.1	1.5×10^{-10}	(29)	2.2×10^{36}
	0.1	2.7×10^{-10}	(29)	4.0×10^{36}
	0.0	1.7×10^{-10}	(29)	2.5×10^{36}
V1974 Cyg	6.3	1.4×10^{-13}	(4)	1.2×10^{32}
	1.7	2.1×10^{-12}	(30)	1.9×10^{33}
	1.4	4.8×10^{-12}	(30)	4.2×10^{33}
	1.1	2.0×10^{-11}	(30)	1.8×10^{34}
	0.7	1.9×10^{-10}	(30)	1.7×10^{35}
	0.5	8.9×10^{-10}	(30)	7.9×10^{35}
HR Del	33.0	1.2×10^{-12}	(4)	1.2×10^{32}
	29.9	7.1×10^{-13}	(4)	7.0×10^{31}
	23.1	1.0×10^{-12}	(2)	9.9×10^{31}
	17.1	3.9×10^{-13}	(4)	3.9×10^{31}
	1.741	4.6×10^{-11}	(3)	4.6×10^{33}
	0.550	1.8×10^{-9}	(3)	1.8×10^{35}
	0.449	1.4×10^{-9}	(3)	1.4×10^{35}
	0.216	5.6×10^{-9}	(3)	5.6×10^{35}
DQ Her	60.4	5.9×10^{-14}	(6)	2.1×10^{30}
	55.7	1.5×10^{-13}	(2)	5.3×10^{30}
	49.8	2.7×10^{-13}	(3)	1.3×10^{31}
	49.7	2.4×10^{-13}	(4)	1.2×10^{31}
	47.5	7.2×10^{-14}	(36)	2.6×10^{30}
	33.0	6×10^{-12}	(37)	2.1×10^{32}
	0.09	1.7×10^{-8}	(34)	6.0×10^{35}
	0.03	1.8×10^{-8}	(34)	6.4×10^{35}
V446 Her	37.3	9.2×10^{-15}	(38)	4.6×10^{30}
V533 Her	35.1	4.5×10^{-14}	(38)	8.6×10^{30}
	33.3	5.6×10^{-14}	(6)	1.1×10^{31}
V838 Her	1.5	1.2×10^{-14}	(40)	4.1×10^{31}
	0.61	1.0×10^{-13}	(40)	3.4×10^{32}
	0.53	1.2×10^{-13}	(40)	4.1×10^{32}
	0.44	1.4×10^{-13}	(13)	4.7×10^{32}
	0.43	2.4×10^{-13}	(40)	8.1×10^{32}
	0.37	3.2×10^{-13}	(40)	1.1×10^{33}
	0.28	7.8×10^{-13}	(13)	2.6×10^{33}
	0.22	1.2×10^{-12}	(13)	4.1×10^{33}
	0.12	5.6×10^{-12}	(13)	1.9×10^{34}
	0.11	1.7×10^{-11}	(40)	5.8×10^{34}
	0.09	2.3×10^{-11}	(13)	7.8×10^{34}
	0.05	1.6×10^{-10}	(40)	5.4×10^{35}
	0.027	5.9×10^{-10}	(13)	2.0×10^{36}
CP Lac	54.1	1.9×10^{-14}	(2)	6.8×10^{30}
	49.7	7.7×10^{-15}	(4)	2.8×10^{30}
	0.42	3.3×10^{-10}	(41)	1.2×10^{35}
	0.32	5.5×10^{-10}	(41)	2.0×10^{35}
	0.26	1.1×10^{-9}	(41)	3.9×10^{35}
	0.18	2.7×10^{-9}	(41)	9.6×10^{35}
	0.13	7.7×10^{-9}	(41)	2.7×10^{36}
	0.10	1.1×10^{-8}	(41)	3.9×10^{36}
	0.07	1.8×10^{-8}	(41)	6.4×10^{36}

Table 3. Hα Flux and Luminosity (continued)

Object	Age (years)	Flux (erg cm^{-2} s^{-1})	Ref.	Luminosity (erg s^{-1})
CP Lac	0.05	2.8×10^{-8}	(41)	1.0×10^{37}
	0.04	3.3×10^{-8}	(41)	1.2×10^{37}
DK Lac	41.4	7.6×10^{-15}	(2)	3.9×10^{31}
	0.24		(42)	1.2×10^{36}
	0.21		(42)	3.7×10^{35}
	0.16		(42)	6.9×10^{35}
	0.12		(42)	8.8×10^{35}
	0.09		(42)	9.0×10^{35}
HY Lup	4.5	1.3×10^{-13}	(4)	9.5×10^{31}
BT Mon	42.2	1.6×10^{-14}	(15)	9.0×10^{30}
GQ Mus	15.2	3.4×10^{-15}	(4)	2.5×10^{31}
	11.1	4.7×10^{-15}	(43)	3.5×10^{31}
	11.05	1.3×10^{-15}	(13)	9.6×10^{30}
	9.01	3.0×10^{-15}	(13)	2.2×10^{31}
	8.64	4.9×10^{-15}	(13)	3.6×10^{31}
	7.51	7.1×10^{-15}	(13)	5.3×10^{31}
	7.36	2.7×10^{-15}	(13)	2.0×10^{31}
	5.39	3.8×10^{-14}	(13)	2.8×10^{32}
V972 Oph	42.8	4.6×10^{-15}	(4)	1.2×10^{31}
	33.8	2.4×10^{-15}	(2)	6.0×10^{30}
V2104 Oph	21.7	1.7×10^{-16}	(4)	
V2214 Oph	13.3	5.3×10^{-15}	(4)	8.5×10^{30}
	2.984	1.2×10^{-13}	(13)	1.2×10^{32}
	2.080	4.3×10^{-13}	(13)	4.3×10^{32}
	1.918	7.0×10^{-13}	(13)	6.9×10^{32}
	1.455	1.0×10^{-12}	(13)	9.9×10^{32}
	1.104	1.3×10^{-12}	(13)	1.3×10^{33}
	1.080	2.0×10^{-11}	(13)	2.0×10^{34}
	0.485	9.8×10^{-11}	(13)	9.7×10^{34}
	0.455	3.0×10^{-10}	(13)	3.0×10^{35}
	0.364	2.1×10^{-10}	(13)	2.1×10^{35}
	0.274	5.9×10^{-10}	(13)	5.8×10^{35}
	0.238	6.3×10^{-10}	(13)	6.2×10^{35}
	0.206	6.8×10^{-10}	(13)	6.7×10^{35}
	0.200	7.5×10^{-10}	(13)	7.4×10^{35}
	0.164	9.8×10^{-10}	(13)	9.7×10^{35}
	0.162	9.6×10^{-10}	(13)	9.5×10^{35}
	0.107	3.0×10^{-10}	(13)	3.0×10^{35}
	0.104	4.3×10^{-10}	(13)	4.3×10^{35}
	0.101	8.7×10^{-11}	(13)	8.6×10^{34}
	0.071	6.7×10^{-10}	(13)	6.6×10^{35}
V2264 Oph	1.301	4.5×10^{-13}	(13)	1.3×10^{34}
	1.088	3.9×10^{-13}	(13)	1.1×10^{34}
	0.904	1.5×10^{-12}	(13)	4.2×10^{34}
	0.397	1.0×10^{-11}	(13)	2.8×10^{35}
	0.232	2.1×10^{-11}	(13)	5.9×10^{35}
	0.173	7.3×10^{-12}	(13)	2.0×10^{35}
	0.118	3.7×10^{-11}	(13)	1.0×10^{36}
	0.077	3.8×10^{-11}	(13)	1.1×10^{36}
	0.041	8.9×10^{-11}	(13)	2.5×10^{36}
	0.027	1.1×10^{-10}	(13)	3.1×10^{36}
GK Per	84.0	1.2×10^{-12}	(4)	6.0×10^{31}
	83.6	1.7×10^{-12}	(3)	8.3×10^{31}
V400 Per	0.46	1.8×10^{-11}	(48)	4.4×10^{35}
	0.45	1.9×10^{-11}	(48)	4.6×10^{35}
	0.35	5.1×10^{-11}	(48)	1.2×10^{36}
	0.28	3.4×10^{-11}	(48)	8.3×10^{35}
	0.24	5.5×10^{-11}	(48)	1.3×10^{36}
	0.20	5.6×10^{-11}	(48)	1.4×10^{36}
RR Pic	72.8	2.4×10^{-13}	(4)	1.1×10^{31}

Table 3. Hα Flux and Luminosity (continued)

Object	Age (years)	Flux (erg cm^{-2} s^{-1})	Ref.	Luminosity (erg s^{-1})
CP Pup	52.9	1.1×10^{-13}	(4)	6.9×10^{31}
V351 Pup	6.1	1.8×10^{-14}	(4)	8.5×10^{31}
	1.325	1.1×10^{-11}	(13)	5.2×10^{34}
	1.3	1.1×10^{-11}	(51)	5.2×10^{34}
	1.237	1.4×10^{-11}	(13)	6.6×10^{34}
	1.2	1.5×10^{-11}	(51)	7.1×10^{34}
	1.011	3.3×10^{-11}	(13)	1.6×10^{35}
	1.0	3.3×10^{-11}	(51)	1.6×10^{35}
	0.915	7.9×10^{-12}	(13)	3.7×10^{34}
	0.375	2.2×10^{-10}	(13)	1.0×10^{36}
	0.189	4.3×10^{-10}	(13)	2.0×10^{36}
	0.112	7.0×10^{-10}	(13)	3.3×10^{36}
	0.088	1.5×10^{-10}	(13)	7.1×10^{35}
	0.030	1.6×10^{-9}	(13)	7.6×10^{36}
V3888 Sgr	23.7	1.5×10^{-15}	(4)	1.2×10^{31}
V4157 Sgr	1.367	3.4×10^{-13}	(13)	1.7×10^{34}
	1.186	4.9×10^{-13}	(13)	2.4×10^{34}
	1.107	5.9×10^{-13}	(13)	2.9×10^{34}
	0.778	1.3×10^{-12}	(13)	6.5×10^{34}
	0.644	2.4×10^{-12}	(13)	1.2×10^{35}
	0.463	8.1×10^{-12}	(13)	4.0×10^{35}
	0.386	5.1×10^{-12}	(13)	2.5×10^{35}
	0.244	1.7×10^{-11}	(13)	8.5×10^{35}
	0.104	7.6×10^{-11}	(13)	3.8×10^{36}
	0.060	1.6×10^{-10}	(13)	8.0×10^{36}
	0.016	3.2×10^{-10}	(13)	1.6×10^{37}
V4160 Sgr	0.197	1.4×10^{-13}	(13)	9.1×10^{32}
	0.096	5.3×10^{-12}	(13)	3.4×10^{34}
	0.008	7.3×10^{-10}	(13)	4.7×10^{36}
V4169 Sgr	0.956	8.5×10^{-13}	(13)	1.0×10^{34}
	0.786	1.7×10^{-12}	(13)	2.0×10^{34}
	0.700	2.5×10^{-12}	(13)	3.0×10^{34}
	0.295	4.9×10^{-11}	(13)	5.8×10^{35}
	0.236	7.3×10^{-11}	(13)	8.6×10^{35}
	0.053	4.0×10^{-10}	(13)	4.6×10^{36}
V4171 Sgr	0.701	4.3×10^{-13}	(13)	3.8×10^{33}
	0.529	1.6×10^{-12}	(13)	1.4×10^{34}
	0.441	4.9×10^{-12}	(13)	4.4×10^{34}
	0.038	4.3×10^{-10}	(13)	3.8×10^{36}
V4444 Sgr	1.2	5.0×10^{-14}	(4)	7.6×10^{32}
V4633 Sgr	2.3	3.6×10^{-13}	(4)	5.7×10^{33}
V4642 Sgr	0.5	3.1×10^{-13}	(4)	1.4×10^{34}
V977 Sco	2.630	6.9×10^{-15}	(13)	2.5×10^{33}
	1.819	3.4×10^{-14}	(13)	1.2×10^{34}
	1.000	1.6×10^{-12}	(13)	5.7×10^{35}
	0.805	1.6×10^{-12}	(13)	5.7×10^{35}
	0.750	1.8×10^{-12}	(13)	6.5×10^{35}
	0.666	2.6×10^{-12}	(13)	9.3×10^{35}
	0.630	2.6×10^{-12}	(13)	9.3×10^{35}
	0.520	3.1×10^{-12}	(13)	1.1×10^{36}
	0.129	4.2×10^{-11}	(13)	1.5×10^{37}
	0.079	3.9×10^{-11}	(13)	1.4×10^{37}
	0.014	2.3×10^{-11}	(13)	8.3×10^{36}
V992 Sco	1.090	1.7×10^{-11}	(13)	2.8×10^{34}
	0.923	2.5×10^{-11}	(13)	4.1×10^{34}
	0.830	2.8×10^{-11}	(13)	4.6×10^{35}
	0.427	9.4×10^{-12}	(13)	1.5×10^{34}
	0.367	5.8×10^{-12}	(13)	9.4×10^{33}
	0.260	5.7×10^{-11}	(13)	9.3×10^{34}
	0.205	2.8×10^{-10}	(13)	4.6×10^{35}

Table 3. Hα Flux and Luminosity (continued)

Object	Age (years)	Flux (erg cm^{-2} s^{-1})	Ref.	Luminosity (erg s^{-1})
V992 Sco	0.186	2.6×10^{-10}	(13)	4.2×10^{35}
	0.181	3.2×10^{-10}	(13)	5.2×10^{35}
	0.175	4.2×10^{-10}	(13)	6.8×10^{35}
	0.164	5.3×10^{-10}	(13)	8.6×10^{35}
	0.159	6.7×10^{-10}	(13)	1.1×10^{36}
	0.153	6.2×10^{-10}	(13)	1.0×10^{36}
	0.137	4.5×10^{-10}	(13)	7.3×10^{35}
	0.131	3.8×10^{-10}	(13)	6.2×10^{35}
	0.126	7.6×10^{-10}	(13)	1.2×10^{36}
	0.121	6.7×10^{-10}	(13)	1.1×10^{36}
	0.115	6.5×10^{-10}	(13)	1.1×10^{36}
	0.110	2.4×10^{-11}	(13)	3.9×10^{34}
	0.104	9.7×10^{-12}	(13)	1.6×10^{34}
	0.099	5.2×10^{-10}	(13)	8.5×10^{35}
	0.077	5.7×10^{-10}	(13)	9.3×10^{35}
	0.046	7.4×10^{-11}	(13)	1.2×10^{35}
	0.033	3.8×10^{-10}	(13)	6.2×10^{35}
	0.022	1.6×10^{-12}	(13)	2.6×10^{33}
V1142 Sco	3.1	2.3×10^{-14}	(4)	2.6×10^{33}
V1142 Sco	1.7	3.4×10^{-14}	(4)	6.5×10^{31}
FV Sct	31.1	2.7×10^{-15}	(2)	
V373 Sct	16.1	6.0×10^{-15}	(2)	3.2×10^{31}
V443 Sct	3.060	9.7×10^{-14}	(13)	1.8×10^{33}
	1.767	3.3×10^{-13}	(13)	6.2×10^{33}
	1.038	2.0×10^{-12}	(13)	3.7×10^{34}
	0.742	5.6×10^{-12}	(13)	1.1×10^{35}
	0.687	4.2×10^{-12}	(13)	7.9×10^{34}
	0.602	1.0×10^{-11}	(13)	1.9×10^{35}
	0.21	3.5×10^{-11}	(54)	6.6×10^{35}
	0.192	7.7×10^{-11}	(13)	1.4×10^{36}
	0.07	6.0×10^{-11}	(54)	1.1×10^{36}
	0.066	1.5×10^{-10}	(13)	2.8×10^{36}
	0.05	1.4×10^{-10}	(54)	2.6×10^{36}
	0.03	3.1×10^{-10}	(54)	5.8×10^{36}
V444 Sct	0.591	3.0×10^{-15}	(13)	1.0×10^{33}
	0.186	8.7×10^{-13}	(13)	3.0×10^{35}
	0.110	4.4×10^{-12}	(13)	1.5×10^{36}
	0.006	7.9×10^{-11}	(13)	2.7×10^{37}
X Ser	97.2	8.8×10^{-15}	(4)	1.7×10^{31}
	96.0	1.3×10^{-14}	(38)	2.6×10^{31}
	94.0	8.6×10^{-15}	(38)	1.7×10^{31}
CT Ser	52.5	3.2×10^{-15}	(4)	7.8×10^{29}
	47.0	7.7×10^{-15}	(6)	1.9×10^{30}
	42.3	1.1×10^{-14}	(2)	2.7×10^{30}
	42.1	1.9×10^{-14}	(55)	5.5×10^{30}
FH Ser	20.5	1.1×10^{-13}	(2)	5.3×10^{31}
	14.5	1.8×10^{-14}	(4)	8.3×10^{30}
LW Ser	22.4	2.9×10^{-15}	(4)	4.6×10^{31}
XX Tau	70.5	3.8×10^{-15}	(4)	1.4×10^{31}
	56.9	1.1×10^{-16}	(4)	4.0×10^{29}
RW UMi	41.7	1.3×10^{-14}	(4)	4.9×10^{31}
	34.7	2.6×10^{-15}	(2)	9.8×10^{30}
	27.9	2.8×10^{-16}	(4)	1.1×10^{30}
LV Vul	23.3	1.4×10^{-14}	(2)	5.2×10^{30}
NQ Vul	21.6	1.7×10^{-14}	(4)	1.3×10^{31}
	14.7	3.6×10^{-14}	(2)	2.7×10^{31}
PW Vul	13.8	1.6×10^{-14}	(4)	2.2×10^{31}
	7.0	1.7×10^{-13}	(2)	2.4×10^{32}
QU Vul	13.5	6.8×10^{-16}	(4)	1.0×10^{30}
	9.5	6.8×10^{-13}	(57)	1.0×10^{33}

Table 3. Hα Flux and Luminosity (continued)

Object	Age (years)	Flux (erg cm^{-2} s^{-1})	Ref.	Luminosity (erg s^{-1})
QU Vul	5.7	1.3×10^{-12}	(59)	1.9×10^{33}
	3.7	3.4×10^{-12}	(59)	5.1×10^{33}
	2.6	8.0×10^{-12}	(59)	1.2×10^{34}
QV Vul	10.5	5.4×10^{-14}	(4)	1.2×10^{32}
	5.71	4.1×10^{-13}	(61)	9.1×10^{32}
	2.79	9.1×10^{-12}	(62)	2.0×10^{34}
	0.02	7.8×10^{-10}	(62)	1.7×10^{36}
recurrent	novae			
V394 CrA	0.077	2.6×10^{-12}	(13)	1.0×10^{34}
	0.058	2.2×10^{-12}	(13)	8.6×10^{33}
	0.021	7.8×10^{-11}	(13)	3.0×10^{35}
	0.015	1.6×10^{-10}	(13)	6.2×10^{35}
T Pyx	31.3	2.0×10^{-13}	(4)	7.6×10^{32}
RS Oph	0.029	2.6×10^{-9}	(67)	5.5×10^{35}
	0.026	2.9×10^{-9}	(67)	6.1×10^{35}
	0.022	2.6×10^{-9}	(67)	5.5×10^{35}
	0.019	5.1×10^{-9}	(67)	1.1×10^{36}
	0.015	6.1×10^{-9}	(67)	1.3×10^{36}
	0.007	4.8×10^{-9}	(67)	1.0×10^{36}
	0.004	3.3×10^{-9}	(67)	7.0×10^{35}
	0.001	2.7×10^{-9}	(67)	5.7×10^{35}
V3890 Sgr	1.937	2.1×10^{-13}	(13)	4.3×10^{33}
	1.044	4.3×10^{-13}	(13)	8.8×10^{33}
	0.501	7.4×10^{-13}	(13)	1.5×10^{34}
	0.411	5.6×10^{-13}	(13)	1.2×10^{34}
	0.241	1.3×10^{-12}	(13)	2.7×10^{34}
	0.183	1.9×10^{-12}	(13)	3.9×10^{34}
	0.112	4.9×10^{-12}	(13)	1.0×10^{35}
	0.093	8.7×10^{-12}	(13)	1.8×10^{35}
	0.077	1.3×10^{-11}	(13)	2.7×10^{35}
	0.049	7.5×10^{-11}	(69)	6.8×10^{35}
	0.014	5.4×10^{-10}	(13)	1.1×10^{37}
U Sco	0.032	1.5×10^{-12}	(71)	3.2×10^{34}
V745 Sco	2.679	4.6×10^{-13}	(13)	3.7×10^{34}
	1.868	6.2×10^{-14}	(13)	5.0×10^{33}
	0.868	1.0×10^{-13}	(13)	8.0×10^{33}
	0.835	8.4×10^{-14}	(13)	6.8×10^{33}
	0.819	3.9×10^{-13}	(13)	3.1×10^{34}
	0.126	2.8×10^{-13}	(13)	2.3×10^{34}
	0.060	6.9×10^{-12}	(13)	5.6×10^{35}
	0.027	9.2×10^{-11}	(13)	7.4×10^{36}
	0.016	2.3×10^{-10}	(13)	1.9×10^{37}
	0.006	3.0×10^{-10}	(13)	2.4×10^{37}
LMC novae				
1988-1	0.088	9.8×10^{-12}	(13)	6.5×10^{36}
	0.047	1.3×10^{-11}	(13)	8.6×10^{36}
	0.022	7.9×10^{-12}	(13)	5.2×10^{36}
1988-2	0.099	3.2×10^{-12}	(13)	2.1×10^{36}
	0.038	1.0×10^{-11}	(13)	6.6×10^{36}
	0.014	1.8×10^{-11}	(13)	1.2×10^{37}
	0.008	2.5×10^{-11}	(13)	1.7×10^{37}
1990-1	0.058	1.7×10^{-12}	(13)	1.2×10^{36}
	0.027	4.2×10^{-12}	(13)	2.8×10^{36}
	0.011	1.5×10^{-11}	(13)	9.9×10^{36}
1990-2	0.025	3.6×10^{-13}	(13)	2.4×10^{35}
1991	0.786	2.7×10^{-14}	(13)	1.8×10^{34}
	0.706	4.0×10^{-14}	(13)	2.6×10^{34}
	0.539	4.5×10^{-14}	(13)	3.0×10^{34}
	0.359	2.0×10^{-13}	(13)	1.3×10^{35}
	0.038	2.2×10^{-11}	(13)	1.5×10^{37}

Table 3. Hα Flux and Luminosity (continued)

Object	Age (years)	Flux (erg cm^{-2} s^{-1})	Ref.	Luminosity (erg s^{-1})
1991	0.003	3.1×10^{-11}	(13)	2.1×10^{37}
1992	0.356	3.2×10^{-13}	(13)	2.1×10^{35}
	0.214	2.6×10^{-12}	(13)	1.7×10^{36}
	0.131	5.3×10^{-12}	(13)	3.5×10^{36}
	0.096	1.4×10^{-11}	(13)	9.2×10^{36}
	0.052	2.6×10^{-11}	(13)	1.7×10^{37}
	0.038	2.2×10^{-11}	(13)	1.5×10^{37}
M31 C-31	0.23	1.7×10^{-14}	(73,74)	4.0×10^{35}
	0.18	2.4×10^{-14}	(73,74)	5.6×10^{35}
	0.05	3.9×10^{-14}	(73,74)	8.9×10^{35}
	0.02	8.0×10^{-14}	(73,74)	1.8×10^{34}
	0.014	8.0×10^{-14}	(73,74)	1.8×10^{34}
	0.008	5.9×10^{-14}	(73,74)	1.4×10^{34}
	0.005	5.9×10^{-14}	(73,74)	1.4×10^{34}
	0.003	6.4×10^{-14}	(73,74)	1.5×10^{34}
C-32	3.72	5.5×10^{-15}	(73,74)	1.3×10^{35}
	3.63	5.1×10^{-15}	(75)	1.5×10^{35}
	3.63	6.7×10^{-15}	(73,74)	1.5×10^{35}
	3.55	7.2×10^{-15}	(73,74)	1.6×10^{35}
	3.47	6.9×10^{-15}	(73,74)	1.6×10^{35}
	2.88	7.3×10^{-15}	(73,74)	1.7×10^{35}
	2.82	8.7×10^{-15}	(73,74)	2.0×10^{35}
	2.69	1.3×10^{-14}	(75)	3.9×10^{35}
	2.63	1.1×10^{-14}	(73,74)	2.6×10^{35}
	2.57	1.1×10^{-14}	(73,74)	2.6×10^{35}
	2.45	1.0×10^{-14}	(73,74)	2.4×10^{35}
	2.00	1.7×10^{-14}	(73,74)	3.8×10^{35}
	1.91	1.5×10^{-14}	(73,74)	3.5×10^{35}
	1.86	1.6×10^{-14}	(73,74)	3.7×10^{35}
	1.78	2.2×10^{-14}	(73,74)	5.0×10^{35}
	1.70	1.9×10^{-14}	(75)	5.7×10^{35}
	1.66	2.4×10^{-14}	(73,74)	5.5×10^{35}
	1.58	2.4×10^{-14}	(73,74)	5.4×10^{35}
	0.74	4.1×10^{-14}	(73,74)	9.4×10^{35}
	0.58	4.1×10^{-14}	(73,74)	9.3×10^{35}
	0.54	3.9×10^{-14}	(73,74)	9.1×10^{35}
	0.50	4.2×10^{-14}	(73,74)	9.6×10^{35}
	0.48	3.8×10^{-14}	(73,74)	8.8×10^{35}
	0.45	3.8×10^{-14}	(73,74)	8.7×10^{35}

[a]flux includes [N II] lines

Table 4. Hβ Flux and Luminosity

Object	Age (years)	Flux (erg cm^{-2} s^{-1})	Ref.	Luminosity (erg s^{-1})
OS And	4.6	6.0×10^{-15}	(2)	4.3×10^{31}
V603 Aql	78.0	5.6×10^{-13}	(6)	9.3×10^{30}
	72.2	6.0×10^{-13}	(2)	1.0×10^{31}
	59.8	1.4×10^{-13}	(6)	2.3×10^{30}
	0.89	7.8×10^{-9}	(7)	1.3×10^{35}
	0.46	2.8×10^{-8}	(7)	4.7×10^{35}
	0.33	9.8×10^{-8}	(7)	1.6×10^{36}
	0.31	1.4×10^{-7}	(7)	2.3×10^{36}
	0.29	1.2×10^{-7}	(7)	2.0×10^{36}
	0.27	1.0×10^{-7}	(7)	1.7×10^{36}
	0.25	1.5×10^{-7}	(7)	2.5×10^{36}
	0.23	1.5×10^{-7}	(7)	2.5×10^{36}
	0.21	1.4×10^{-7}	(7)	2.3×10^{36}
	0.19	1.4×10^{-7}	(7)	2.3×10^{36}
	0.18	1.6×10^{-7}	(7)	2.7×10^{36}
	0.17	2.4×10^{-7}	(7)	4.0×10^{36}
	0.16	1.9×10^{-7}	(7)	3.2×10^{36}
	0.15	2.4×10^{-7}	(7)	4.0×10^{36}
	0.14	2.9×10^{-7}	(7)	4.8×10^{36}
	0.13	2.3×10^{-7}	(7)	3.8×10^{36}
	0.12	2.1×10^{-7}	(7)	3.5×10^{35}
	0.09	2.4×10^{-7}	(7)	4.0×10^{36}
	0.07	1.4×10^{-7}	(7)	2.3×10^{36}
	0.06	3.0×10^{-7}	(7)	5.0×10^{36}
	0.04	4.0×10^{-7}	(7)	6.6×10^{36}
	0.03	7.6×10^{-7}	(7)	1.3×10^{37}
	0.02	6.6×10^{-7}	(7)	1.1×10^{37}
	0.01	1.2×10^{-6}	(7)	2.0×10^{37}
V1370 Aql	0.43	5.1×10^{-13}	(10)	1.1×10^{34}
V1419 Aql	0.118	4.7×10^{-12}	(13)	5.8×10^{34}
V1425 Aql	2.31	1.3×10^{-14}	(14)	1.4×10^{32}
	0.31	7.0×10^{-12}	(14)	7.6×10^{34}
	0.20	2.8×10^{-11}	(14)	3.0×10^{35}
	0.14	3.0×10^{-11}	(14)	3.2×10^{35}
	0.14	2.3×10^{-11}	(14)	2.5×10^{35}
V705 Cas	0.186	8.5×10^{-13}	(13)	5.6×10^{33}
	0.184	1.0×10^{-12}	(13)	6.6×10^{33}
	0.176	1.2×10^{-11}	(13)	7.9×10^{34}
V842 Cen	1.3	5.9×10^{-13}	(22)	5.8×10^{32}
	0.7	2.8×10^{-12}	(22)	2.8×10^{33}
	0.6	5.8×10^{-12}	(22)	5.7×10^{33}
V868 Cen	2.060	1.5×10^{-14}	(13)	2.1×10^{33}
	1.975	1.9×10^{-14}	(13)	2.6×10^{33}
	1.830	2.8×10^{-14}	(13)	3.8×10^{33}
	1.328	1.0×10^{-13}	(13)	1.4×10^{34}
	0.925	3.1×10^{-13}	(13)	4.2×10^{34}
	0.767	6.7×10^{-13}	(13)	9.2×10^{34}
	0.263	7.0×10^{-13}	(13)	9.6×10^{34}
	0.194	3.1×10^{-13}	(13)	4.2×10^{35}
	0.112	3.1×10^{-12}	(13)	4.2×10^{35}
	0.099	6.9×10^{-12}	(13)	9.5×10^{35}
	0.082	3.2×10^{-12}	(13)	4.4×10^{35}
	0.063	4.2×10^{-12}	(13)	5.8×10^{35}
	0.049	4.8×10^{-12}	(13)	6.6×10^{35}
	0.003	1.6×10^{-12}	(13)	2.2×10^{35}
IV Cep	0.31	4.0×10^{-12}	(25)	1.1×10^{35}
	0.21	9.4×10^{-12}	(25)	2.6×10^{35}
	0.09	1.5×10^{-11}	(25)	4.1×10^{35}
	0.05	2.1×10^{-11}	(25)	5.8×10^{35}
V476 Cyg	42.2	5.1×10^{-15}	(2)	3.9×10^{30}

Table 4. Hβ Flux and Luminosity (continued)

Object	Age (years)	Flux (erg cm^{-2} s^{-1})	Ref.	Luminosity (erg s^{-1})
V476 Cyg	0.15	2.3×10^{-9}	(7)	1.7×10^{36}
	0.13	4.4×10^{-9}	(7)	3.3×10^{36}
	0.12	4.7×10^{-9}	(7)	3.6×10^{36}
	0.11	8.1×10^{-9}	(7)	6.1×10^{36}
	0.09	1.0×10^{-8}	(7)	7.6×10^{36}
	0.08	1.6×10^{-8}	(7)	1.2×10^{37}
	0.07	2.3×10^{-8}	(7)	1.7×10^{37}
	0.06	4.0×10^{-8}	(7)	3.0×10^{37}
	0.04	8.6×10^{-8}	(7)	6.5×10^{37}
	0.03	7.1×10^{-8}	(7)	5.4×10^{37}
	0.02	8.4×10^{-8}	(7)	6.3×10^{37}
	0.01	8.6×10^{-8}	(7)	6.5×10^{37}
V1500 Cyg	14.9	6.9×10^{-15}	(2)	1.0×10^{31}
	0.98	2.7×10^{-12}	(28)	3.9×10^{33}
	0.81	3.2×10^{-12}	(28)	4.6×10^{33}
	0.73	6.9×10^{-12}	(28)	1.0×10^{34}
	0.38	1.5×10^{-11}	(28)	2.2×10^{34}
	0.33	2.4×10^{-11}	(28)	3.5×10^{34}
	0.28	3.7×10^{-11}	(28)	5.3×10^{34}
	0.24	5.8×10^{-11}	(28)	8.4×10^{34}
	0.22	8.6×10^{-11}	(28)	1.2×10^{35}
	0.19	1.1×10^{-10}	(28)	1.6×10^{35}
	0.17	1.5×10^{-10}	(28)	2.2×10^{35}
	0.15	2.1×10^{-10}	(28)	3.0×10^{35}
	0.13	3.1×10^{-10}	(28)	4.5×10^{35}
	0.11	3.7×10^{-10}	(28)	5.3×10^{35}
	0.10	5.1×10^{-10}	(28)	7.4×10^{35}
	0.07	8.4×10^{-10}	(28)	1.2×10^{36}
	0.05	1.5×10^{-9}	(28)	2.2×10^{36}
	0.03	5.3×10^{-9}	(28)	7.7×10^{36}
	0.01	1.7×10^{-8}	(28)	2.5×10^{37}
	0.01	1.1×10^{-9}	(28)	1.6×10^{36}
V1819 Cyg	1.8	8.0×10^{-14}	(29)	1.8×10^{33}
	0.9	3.5×10^{-12}	(29)	7.8×10^{34}
	0.3	3.1×10^{-12}	(29)	6.9×10^{34}
	0.3	1.2×10^{-12}	(29)	2.7×10^{34}
	0.2	4.9×10^{-12}	(29)	1.1×10^{35}
	0.2	5.0×10^{-12}	(29)	1.1×10^{35}
	0.2	1.3×10^{-11}	(29)	2.9×10^{35}
	0.1	1.1×10^{-11}	(29)	2.4×10^{35}
	0.1	1.4×10^{-11}	(29)	3.1×10^{35}
	0.1	2.1×10^{-11}	(29)	4.7×10^{35}
	0.1	3.2×10^{-11}	(29)	7.1×10^{35}
	0.0	3.5×10^{-11}	(29)	7.8×10^{35}
V1974 Cyg	1.8	4.5×10^{-13}	(30)	5.5×10^{32}
	1.7	6.0×10^{-13}	(30)	7.4×10^{32}
	1.4	1.3×10^{-12}	(30)	1.6×10^{33}
	1.2	4.1×10^{-12}	(30)	5.0×10^{33}
	1.1	6.4×10^{-12}	(30)	7.9×10^{33}
	0.7	4.4×10^{-11}	(30)	5.4×10^{34}
	0.5	1.0×10^{-10}	(30)	1.2×10^{35}
	0.5	1.7×10^{-10}	(30)	2.1×10^{35}
	0.4	2.3×10^{-10}	(30)	2.8×10^{35}
	0.2	3.9×10^{-10}	(30)	4.8×10^{35}
HR Del	23.1	2.1×10^{-13}	(2)	2.4×10^{31}
	10.8	3.9×10^{-13}	(6)	4.5×10^{31}
	8.1	7.5×10^{-13}	(32)	8.6×10^{31}
	4.9	3.5×10^{-11}	(31)	4.0×10^{33}
	4.684	3.3×10^{-12}	(3)	3.8×10^{32}
	3.702	1.3×10^{-11}	(3)	1.5×10^{33}

Table 4. Hβ Flux and Luminosity (continued)

Object	Age (years)	Flux (erg cm^{-2} s^{-1})	Ref.	Luminosity (erg s^{-1})
HR Del	2.0	6.5×10^{-10}	(31)	7.5×10^{34}
	1.741	7.3×10^{-11}	(3)	8.4×10^{33}
	1.667	1.1×10^{-10}	(3)	1.3×10^{34}
	0.964	5.2×10^{-10}	(3)	5.9×10^{34}
	0.550	1.0×10^{-9}	(3)	1.2×10^{35}
	0.449	1.0×10^{-9}	(3)	1.2×10^{35}
	0.216	2.6×10^{-9}	(3)	2.9×10^{35}
DQ Her	60.4	9.1×10^{-14}	(6)	3.6×10^{30}
	55.7	1.0×10^{-13}	(2)	3.9×10^{30}
	47.5	4.5×10^{-14}	(35)	1.8×10^{30}
	43.3	8.7×10^{-14}	(6)	3.4×10^{30}
	1.69	1.7×10^{-10}	(34)	6.7×10^{33}
	0.84	9.2×10^{-10}	(34)	3.6×10^{34}
	0.60	1.2×10^{-9}	(34)	4.7×10^{34}
	0.54	1.1×10^{-9}	(34)	4.3×10^{34}
	0.44	2.7×10^{-10}	(34)	1.1×10^{34}
	0.23	4.4×10^{-9}	(34)	1.7×10^{35}
	0.19	8.4×10^{-9}	(34)	3.3×10^{35}
	0.09	1.1×10^{-8}	(34)	4.3×10^{35}
	0.03	1.6×10^{-8}	(34)	6.3×10^{35}
V446 Her	37.3	8.0×10^{-15}	(38)	5.6×10^{30}
V533 Her	35.1	3.5×10^{-14}	(38)	6.7×10^{30}
	33.3	5.4×10^{-14}	(6)	1.0×10^{31}
	15.2	2.2×10^{-14}	(6)	4.2×10^{30}
V838 Her	0.61	1.5×10^{-14}	(40)	8.3×10^{31}
	0.53	1.8×10^{-14}	(40)	9.9×10^{31}
	0.44	1.9×10^{-14}	(13)	1.1×10^{32}
	0.42	4.1×10^{-14}	(40)	2.3×10^{32}
	0.37	7.0×10^{-14}	(40)	3.9×10^{32}
	0.28	1.5×10^{-13}	(13)	8.3×10^{32}
	0.22	2.4×10^{-13}	(13)	1.3×10^{33}
	0.12	1.1×10^{-12}	(13)	6.1×10^{33}
	0.11	3.4×10^{-12}	(40)	1.9×10^{34}
	0.088	3.8×10^{-12}	(13)	2.1×10^{34}
	0.05	2.6×10^{-11}	(40)	1.4×10^{35}
	0.027	7.2×10^{-11}	(13)	4.0×10^{35}
CP Lac	54.1	1.1×10^{-14}	(2)	4.8×10^{30}
	43.3	3.6×10^{-15}	(6)	1.6×10^{30}
DK Lac	41.4	4.0×10^{-15}	(2)	3.2×10^{31}
	29.8	4.0×10^{-15}	(6)	3.2×10^{31}
	0.34		(42)	8.1×10^{34}
	0.30		(42)	7.4×10^{34}
	0.28		(42)	7.4×10^{34}
	0.24		(42)	2.6×10^{35}
	0.21		(42)	1.8×10^{35}
	0.16		(42)	2.8×10^{35}
	0.12		(42)	2.2×10^{35}
	0.09		(42)	2.0×10^{35}
GQ Mus	11.1	1.8×10^{-15}	(43)	2.0×10^{31}
	11.05	4.1×10^{-16}	(13)	4.6×10^{30}
	9.01	6.9×10^{-16}	(13)	7.7×10^{30}
	8.64	7.2×10^{-16}	(13)	8.1×10^{30}
	7.51	1.8×10^{-15}	(13)	2.0×10^{31}
	7.5	6.4×10^{-15}	(45)	7.2×10^{31}
	7.36	1.4×10^{-15}	(13)	1.6×10^{31}
	5.4	6.0×10^{-14}	(45)	6.7×10^{32}
	5.39	1.1×10^{-14}	(13)	1.2×10^{32}
	4.4	1.2×10^{-13}	(45)	1.3×10^{33}
	4.0	2.1×10^{-13}	(45)	2.4×10^{33}
	3.4	6.6×10^{-13}	(45)	7.4×10^{33}

Table 4. Hβ Flux and Luminosity (continued)

Object	Age (years)	Flux (erg cm^{-2} s^{-1})	Ref.	Luminosity (erg s^{-1})
GQ Mus	3.1	1.1×10^{-12}	(45)	1.2×10^{34}
	3.0	1.4×10^{-12}	(45)	1.6×10^{34}
	2.3	6.8×10^{-12}	(45)	7.6×10^{34}
	2.3	7.6×10^{-12}	(45)	8.5×10^{34}
	1.5	5.1×10^{-11}	(45)	5.7×10^{35}
	1.4	6.3×10^{-11}	(45)	7.1×10^{35}
	1.2	8.7×10^{-11}	(45)	9.8×10^{35}
	1.2	8.3×10^{-11}	(45)	9.3×10^{35}
V2214 Oph	2.984	2.3×10^{-14}	(13)	3.7×10^{31}
	2.080	8.3×10^{-14}	(13)	1.4×10^{32}
	1.918	1.0×10^{-13}	(13)	1.6×10^{32}
	1.455	2.1×10^{-13}	(13)	3.4×10^{32}
	1.104	2.2×10^{-13}	(13)	3.6×10^{32}
	1.080	3.3×10^{-12}	(13)	5.4×10^{33}
	0.485	1.0×10^{-11}	(13)	1.6×10^{34}
	0.455	1.1×10^{-11}	(13)	1.8×10^{34}
	0.364	1.1×10^{-11}	(13)	1.8×10^{34}
	0.277	8.8×10^{-11}	(13)	1.4×10^{35}
	0.274	1.8×10^{-11}	(13)	2.9×10^{34}
	0.246	1.9×10^{-11}	(13)	3.1×10^{34}
	0.241	2.2×10^{-11}	(13)	3.6×10^{34}
	0.238	2.3×10^{-11}	(13)	3.7×10^{34}
	0.206	3.2×10^{-11}	(13)	5.2×10^{34}
	0.200	3.2×10^{-11}	(13)	5.2×10^{34}
	0.162	5.5×10^{-11}	(13)	8.9×10^{34}
	0.107	2.9×10^{-11}	(13)	4.7×10^{34}
	0.104	3.1×10^{-11}	(13)	5.0×10^{34}
	0.101	2.7×10^{-11}	(13)	4.4×10^{34}
	0.071	6.4×10^{-11}	(13)	1.0×10^{34}
V2264 Oph	1.301	4.6×10^{-14}	(13)	2.8×10^{33}
	1.088	4.8×10^{-14}	(13)	3.0×10^{33}
	0.904	1.6×10^{-13}	(13)	9.9×10^{33}
	0.397	8.2×10^{-13}	(13)	5.1×10^{34}
	0.232	1.3×10^{-12}	(13)	8.0×10^{34}
	0.173	4.3×10^{-13}	(13)	2.7×10^{34}
	0.118	1.7×10^{-12}	(13)	1.1×10^{35}
	0.077	2.1×10^{-12}	(13)	1.3×10^{35}
	0.041	7.2×10^{-12}	(13)	4.5×10^{35}
	0.027	9.9×10^{-12}	(13)	6.1×10^{35}
GK Per	78.7	1.2×10^{-13}	(6)	8.1×10^{30}
	1.44	1.6×10^{-10}	(7)	1.1×10^{34}
	0.74	4.0×10^{-10}	(7)	2.7×10^{34}
	0.57	1.5×10^{-9}	(7)	1.0×10^{35}
	0.48	1.9×10^{-9}	(7)	1.3×10^{35}
	0.39	3.1×10^{-9}	(7)	2.1×10^{35}
	0.34	3.1×10^{-9}	(7)	2.1×10^{35}
	0.29	7.4×10^{-9}	(7)	5.0×10^{35}
	0.17	1.6×10^{-8}	(7)	1.1×10^{36}
	0.11	2.1×10^{-8}	(7)	1.4×10^{36}
	0.07	2.1×10^{-8}	(7)	1.4×10^{36}
	0.06	3.3×10^{-8}	(7)	2.2×10^{36}
	0.04	5.8×10^{-8}	(7)	3.9×10^{36}
	0.01	2.2×10^{-7}	(7)	1.5×10^{37}
V400 Per	0.46	5.5×10^{-12}	(48)	1.4×10^{35}
	0.45	5.8×10^{-12}	(48)	1.5×10^{35}
	0.35	1.2×10^{-11}	(48)	3.1×10^{35}
	0.28	1.1×10^{-11}	(48)	2.9×10^{35}
	0.24	1.4×10^{-11}	(48)	3.6×10^{35}
	0.20	1.7×10^{-11}	(48)	4.4×10^{35}

Table 4. Hβ Flux and Luminosity (continued)

Object	Age (years)	Flux (erg cm^{-2} s^{-1})	Ref.	Luminosity (erg s^{-1})
RR Pic	3.66	7.7×10^{-10}	(49)	3.7×10^{34}
	2.86	2.5×10^{-9}	(49)	1.2×10^{35}
	2.56	2.8×10^{-9}	(49)	1.4×10^{35}
	1.87	3.6×10^{-9}	(49)	1.8×10^{35}
	1.79	4.0×10^{-9}	(49)	1.9×10^{35}
	1.75	2.2×10^{-9}	(49)	1.1×10^{35}
	1.49	5.4×10^{-9}	(49)	2.6×10^{35}
	1.38	6.9×10^{-9}	(49)	3.4×10^{35}
	1.32	5.3×10^{-9}	(49)	2.6×10^{35}
	1.25	7.7×10^{-9}	(49)	3.7×10^{35}
	1.15	1.6×10^{-8}	(49)	7.8×10^{35}
	0.99	1.6×10^{-8}	(49)	7.8×10^{35}
	0.95	1.1×10^{-8}	(49)	5.3×10^{35}
	0.91	1.1×10^{-8}	(49)	5.3×10^{35}
	0.88	7.3×10^{-9}	(49)	3.5×10^{35}
	0.85	8.4×10^{-9}	(49)	4.1×10^{35}
	0.78	1.2×10^{-8}	(49)	5.8×10^{35}
	0.74	1.7×10^{-8}	(49)	8.3×10^{35}
	0.66	2.0×10^{-8}	(49)	9.7×10^{35}
	0.62	2.2×10^{-8}	(49)	1.1×10^{36}
	0.59	2.1×10^{-8}	(49)	1.0×10^{36}
	0.55	1.5×10^{-8}	(49)	7.3×10^{35}
	0.50	2.0×10^{-8}	(49)	9.7×10^{35}
	0.46	1.6×10^{-8}	(49)	7.8×10^{35}
	0.44	1.9×10^{-8}	(49)	9.2×10^{35}
	0.42	1.6×10^{-8}	(49)	7.8×10^{35}
	0.36	1.6×10^{-8}	(49)	7.8×10^{35}
	0.28	1.9×10^{-8}	(49)	9.2×10^{35}
	0.23	3.3×10^{-8}	(49)	1.6×10^{36}
	0.15	3.8×10^{-8}	(49)	1.8×10^{36}
	0.04	7.0×10^{-8}	(49)	3.4×10^{36}
	0.02	9.0×10^{-8}	(49)	4.4×10^{36}
	0.01	8.1×10^{-8}	(49)	3.9×10^{36}
V351 Pup	1.325	1.8×10^{-12}	(13)	1.7×10^{34}
	1.3	1.7×10^{-12}	(51)	1.6×10^{34}
	1.237	2.5×10^{-12}	(13)	2.4×10^{34}
	1.2	2.3×10^{-12}	(51)	2.2×10^{34}
	1.011	5.0×10^{-12}	(13)	4.8×10^{34}
	1.0	4.8×10^{-12}	(51)	4.6×10^{34}
	0.375	2.8×10^{-11}	(13)	2.7×10^{35}
	0.189	4.3×10^{-11}	(13)	4.2×10^{35}
	0.112	1.1×10^{-11}	(13)	1.1×10^{35}
	0.088	1.1×10^{-11}	(13)	1.1×10^{35}
	0.030	1.4×10^{-10}	(13)	1.4×10^{36}
V4157 Sgr	1.367	3.9×10^{-14}	(13)	4.8×10^{33}
	1.186	4.4×10^{-14}	(13)	5.5×10^{33}
	1.107	4.4×10^{-14}	(13)	5.5×10^{33}
	0.778	6.7×10^{-14}	(13)	8.3×10^{33}
	0.644	1.5×10^{-13}	(13)	1.9×10^{34}
	0.463	8.5×10^{-13}	(13)	1.1×10^{35}
	0.386	4.7×10^{-13}	(13)	5.8×10^{34}
	0.244	1.4×10^{-12}	(13)	1.7×10^{35}
	0.104	5.7×10^{-12}	(13)	7.1×10^{35}
	0.060	9.9×10^{-12}	(13)	1.2×10^{36}
	0.016	3.2×10^{-11}	(13)	4.0×10^{36}
V4160 Sgr	0.197	absent	(13)	
	0.096	6.0×10^{-13}	(13)	5.2×10^{33}
	0.008	1.1×10^{-10}	(13)	9.6×10^{35}
V4169 Sgr	0.956	1.1×10^{-13}	(13)	1.9×10^{33}
	0.786	2.4×10^{-13}	(13)	4.0×10^{33}

Table 4. Hβ Flux and Luminosity (continued)

Object	Age (years)	Flux (erg cm^{-2} s^{-1})	Ref.	Luminosity (erg s^{-1})
V4169 Sgr	0.700	4.0×10^{-13}	(13)	6.7×10^{33}
	0.295	7.0×10^{-12}	(13)	1.2×10^{35}
	0.053	5.1×10^{-11}	(13)	8.6×10^{35}
V4171 Sgr	0.701	8.4×10^{-14}	(13)	1.4×10^{33}
	0.529	2.7×10^{-13}	(13)	4.3×10^{33}
	0.441	4.4×10^{-13}	(13)	7.1×10^{33}
	0.110	1.1×10^{-11}	(13)	1.8×10^{35}
	0.038	5.4×10^{-11}	(13)	8.7×10^{35}
V977 Sco	1.819	1.6×10^{-13}	(13)	5.7×10^{34}
	1.000	1.6×10^{-13}	(13)	5.7×10^{34}
	0.805	1.4×10^{-13}	(13)	5.0×10^{34}
	0.750	1.5×10^{-13}	(13)	5.4×10^{34}
	0.666	2.1×10^{-13}	(13)	7.5×10^{34}
	0.630	2.2×10^{-13}	(13)	7.9×10^{34}
	0.520	2.7×10^{-13}	(13)	9.7×10^{34}
	0.129	1.6×10^{-12}	(13)	5.7×10^{35}
	0.079	1.0×10^{-12}	(13)	3.6×10^{35}
	0.014	2.4×10^{-12}	(13)	8.6×10^{35}
V992 Sco	1.090	1.3×10^{-12}	(13)	2.1×10^{33}
	0.923	2.1×10^{-12}	(13)	3.4×10^{33}
	0.830	2.6×10^{-12}	(13)	4.2×10^{33}
	0.427	4.6×10^{-13}	(13)	7.5×10^{32}
	0.205	3.6×10^{-11}	(13)	5.9×10^{34}
	0.186	2.8×10^{-11}	(13)	4.6×10^{34}
	0.181	2.5×10^{-11}	(13)	4.1×10^{34}
	0.175	2.2×10^{-11}	(13)	3.6×10^{34}
	0.164	3.7×10^{-11}	(13)	6.0×10^{34}
	0.159	3.9×10^{-11}	(13)	6.3×10^{34}
	0.153	5.0×10^{-11}	(13)	8.1×10^{34}
	0.137	3.7×10^{-11}	(13)	6.0×10^{34}
	0.131	1.8×10^{-11}	(13)	2.9×10^{34}
	0.126	6.2×10^{-11}	(13)	1.0×10^{35}
	0.121	6.1×10^{-11}	(13)	9.9×10^{34}
	0.115	6.9×10^{-11}	(13)	1.1×10^{35}
	0.110	2.9×10^{-12}	(13)	4.7×10^{33}
	0.104	1.1×10^{-12}	(13)	1.8×10^{33}
	0.099	4.1×10^{-11}	(13)	6.7×10^{34}
	0.077	3.9×10^{-11}	(13)	6.3×10^{34}
	0.046	3.2×10^{-12}	(13)	5.2×10^{33}
	0.033	4.2×10^{-11}	(13)	6.8×10^{34}
	0.022	2.3×10^{-13}	(13)	3.7×10^{32}
V443 Sct	3.060	6.0×10^{-15}	(13)	1.7×10^{32}
	1.767	2.4×10^{-14}	(13)	6.9×10^{32}
	1.038	2.1×10^{-13}	(13)	6.1×10^{33}
	0.742	6.6×10^{-13}	(13)	1.9×10^{34}
	0.687	5.4×10^{-13}	(13)	1.6×10^{34}
	0.602	1.2×10^{-12}	(13)	3.5×10^{34}
	0.21	2.3×10^{-12}	(54)	4.5×10^{34}
	0.192	3.2×10^{-12}	(13)	9.3×10^{34}
	0.07	8.4×10^{-12}	(54)	1.7×10^{35}
	0.066	2.7×10^{-11}	(13)	7.8×10^{35}
	0.05	1.1×10^{-11}	(54)	2.2×10^{35}
	0.03	2.8×10^{-11}	(54)	5.5×10^{35}

Table 4. Hβ Flux and Luminosity (continued)

Object	Age (years)	Flux (erg cm^{-2} s^{-1})	Ref.	Luminosity (erg s^{-1})
V444 Sct	0.186	5.7×10^{-14}	(13)	2.0×10^{34}
	0.110	2.8×10^{-13}	(13)	9.7×10^{34}
	0.006	1.2×10^{-11}	(13)	4.1×10^{35}
X Ser	96.0	5.4×10^{-15}	(38)	1.4×10^{31}
	94.0	4.5×10^{-15}	(38)	1.1×10^{31}
	86.9	8.0×10^{-15}	(55)	2.0×10^{31}
	74.8	4.9×10^{-15}	(6)	1.2×10^{31}
CT Ser	42.3	8.2×10^{-15}	(2)	2.0×10^{30}
FH Ser	20.5	1.2×10^{-14}	(2)	1.1×10^{31}
	9.7	1.8×10^{-14}	(6)	1.6×10^{31}
RW UMi	32.6	2.0×10^{-15}	(55)	8.3×10^{30}
LV Vul	23.3	5.0×10^{-15}	(2)	3.2×10^{30}
NQ Vul	14.7	5.0×10^{-15}	(2)	7.3×10^{30}
PW Vul	2.8	7.7×10^{-14}	(58)	1.9×10^{32}
	1.9	2.6×10^{-13}	(58)	6.3×10^{32}
	1.7	2.8×10^{-13}	(58)	6.7×10^{32}
	1.1	2.6×10^{-12}	(58)	6.3×10^{33}
	0.8	5.9×10^{-12}	(58)	1.4×10^{34}
	0.6	1.7×10^{-11}	(58)	4.1×10^{34}
QU Vul	9.5	2.1×10^{-13}	(57)	5.6×10^{32}
	5.7	2.8×10^{-13}	(59)	7.5×10^{32}
	3.7	5.5×10^{-13}	(59)	1.5×10^{33}
	2.92	9.4×10^{-14}	(60)	2.5×10^{32}
	2.83	1.6×10^{-13}	(60)	4.2×10^{32}
	2.70	2.2×10^{-13}	(60)	5.9×10^{32}
	2.6	1.2×10^{-12}	(59)	3.2×10^{33}
	2.51	2.4×10^{-13}	(60)	6.4×10^{32}
	2.41	2.6×10^{-13}	(60)	7.0×10^{32}
	2.36	2.9×10^{-13}	(60)	7.8×10^{32}
	2.25	4.6×10^{-13}	(60)	1.2×10^{33}
	1.79	9.5×10^{-13}	(60)	2.6×10^{33}
	1.78	8.2×10^{-13}	(60)	2.2×10^{33}
	1.75	8.4×10^{-13}	(60)	2.3×10^{33}
	1.68	1.4×10^{-12}	(60)	3.8×10^{33}
	1.59	1.6×10^{-12}	(60)	4.2×10^{33}
	1.54	1.6×10^{-12}	(60)	4.3×10^{33}
	1.45	2.0×10^{-12}	(60)	5.2×10^{33}
	1.32	1.9×10^{-12}	(60)	5.2×10^{33}
	0.85	4.6×10^{-12}	(60)	1.2×10^{34}
	0.71	7.4×10^{-12}	(60)	2.0×10^{34}
	0.39	9.7×10^{-12}	(60)	2.6×10^{34}
QV Vul	5.71	2.6×10^{-14}	(61)	8.6×10^{31}
	2.79	7.3×10^{-13}	(62)	2.4×10^{33}
	0.02	1.9×10^{-10}	(62)	6.3×10^{35}
recurrent	novae			
V394 CrA	0.077	6.0×10^{-13}	(13)	3.0×10^{33}
	0.058	4.5×10^{-13}	(13)	2.2×10^{33}
	0.021	2.1×10^{-11}	(13)	1.1×10^{35}
	0.015	3.9×10^{-11}	(13)	1.9×10^{35}
RS Oph	0.551	3.0×10^{-12}	(66)	1.3×10^{33}
	0.118	8.2×10^{-11}	(67)	3.6×10^{34}
	0.107	8.9×10^{-11}	(67)	3.9×10^{34}
	0.091	7.2×10^{-11}	(67)	3.1×10^{34}
	0.074	9.6×10^{-11}	(67)	4.2×10^{34}
	0.069	2.2×10^{-10}	(67)	9.6×10^{34}
	0.042	1.5×10^{-10}	(67)	6.5×10^{34}
	0.039	3.3×10^{-10}	(67)	1.4×10^{35}
	0.037	3.6×10^{-10}	(67)	1.6×10^{35}
	0.029	3.1×10^{-10}	(67)	1.4×10^{35}
	0.028	1.9×10^{-10}	(67)	8.3×10^{34}

Table 4. Hβ Flux and Luminosity (continued)

Object	Age (years)	Flux (erg cm^{-2} s^{-1})	Ref.	Luminosity (erg s^{-1})
RS Oph	0.020	6.4×10^{-10}	(67)	2.8×10^{35}
	0.015	1.0×10^{-9}	(67)	4.4×10^{35}
	0.007	2.6×10^{-9}	(67)	1.1×10^{36}
	0.004	3.3×10^{-9}	(67)	1.4×10^{36}
	0.001	2.6×10^{-9}	(67)	1.1×10^{36}
V3890 Sgr	1.937	1.8×10^{-14}	(13)	1.1×10^{33}
	1.044	3.9×10^{-14}	(13)	2.4×10^{33}
	0.501	9.2×10^{-14}	(13)	5.7×10^{33}
	0.411	6.3×10^{-14}	(13)	3.9×10^{33}
	0.241	1.4×10^{-13}	(13)	8.7×10^{33}
	0.183	1.8×10^{-13}	(13)	1.1×10^{34}
	0.112	4.2×10^{-13}	(13)	2.6×10^{34}
	0.093	8.5×10^{-13}	(13)	5.3×10^{34}
	0.077	1.2×10^{-12}	(13)	7.4×10^{34}
	0.049	8.2×10^{-12}	(69)	1.6×10^{34}
	0.014	7.5×10^{-11}	(13)	4.6×10^{36}
U Sco	0.032	6.1×10^{-11}	(71)	2.3×10^{36}
V745 Sco	2.679	2.2×10^{-14}	(13)	4.8×10^{33}
	1.868	1.7×10^{-15}	(13)	3.7×10^{32}
	0.868	5.9×10^{-15}	(13)	1.3×10^{33}
	0.835	4.2×10^{-15}	(13)	9.2×10^{32}
	0.819	$2,0 \times 10^{-14}$	(13)	4.4×10^{33}
	0.126	1.2×10^{-14}	(13)	2.6×10^{33}
	0.060	2.8×10^{-13}	(13)	6.1×10^{34}
	0.027	2.8×10^{-12}	(13)	6.1×10^{35}
	0.016	1.1×10^{-11}	(13)	2.4×10^{36}
	0.006	3.0×10^{-11}	(13)	6.6×10^{36}
LMC novae				
1988-1	0.088	1.1×10^{-12}	(13)	9.3×10^{35}
	0.047	3.3×10^{-12}	(13)	2.8×10^{36}
	0.022	2.8×10^{-12}	(13)	2.4×10^{36}
1988-2	0.099	6.6×10^{-13}	(13)	5.6×10^{35}
	0.038	1.8×10^{-12}	(13)	1.5×10^{36}
	0.014	4.6×10^{-12}	(13)	3.9×10^{36}
	0.008	1.2×10^{-11}	(13)	1.0×10^{37}
1990-1	0.058	4.4×10^{-13}	(13)	3.7×10^{35}
	0.027	1.0×10^{-12}	(13)	8.5×10^{35}
	0.011	3.1×10^{-12}	(13)	2.6×10^{36}
1990-2	0.025	9.7×10^{-14}	(13)	8.2×10^{34}
1991	0.786	7.7×10^{-15}	(13)	6.5×10^{33}
	0.706	1.2×10^{-14}	(13)	1.0×10^{34}
	0.539	9.0×10^{-15}	(13)	7.6×10^{33}
	0.359	5.0×10^{-14}	(13)	4.2×10^{34}
	0.038	3.6×10^{-12}	(13)	3.1×10^{36}
	0.003	2.2×10^{-11}	(13)	1.9×10^{37}
1992	0.356	7.2×10^{-14}	(13)	6.1×10^{34}
	0.214	4.1×10^{-12}	(13)	3.5×10^{36}
	0.131	7.1×10^{-13}	(13)	6.0×10^{35}
	0.096	1.9×10^{-12}	(13)	1.6×10^{36}
	0.038	4.0×10^{-12}	(13)	3.4×10^{36}
M32 novae				
C-32	4.7	9.2×10^{-16}	(75)	2.3×10^{34}
	3.6	1.12×10^{-15}	(75)	2.9×10^{34}
	2.7	1.96×10^{-15}	(75)	5.0×10^{34}
	1.7	2.12×10^{-15}	(75)	5.4×10^{34}